Meteoritics & Planetary Science 42, Nr 4/5, 591–609 (2007)
Abstract available online at http://meteoritics.org

Shock-metamorphic petrography and microRaman spectroscopy of quartz in upper impactite interval, ICDP drill core LB-07A, Bosumtwi impact crater, Ghana

Jared R. MORROW

Department of Geological Sciences, San Diego State University, 5500 Campanile Drive, San Diego, California 92182–1020, USA
E-mail: jmorrow@geology.sdsu.edu

(Received 10 October 2006; revision accepted 23 December 2006)

Abstract–Standard and universal stage optical microscope and microRaman spectroscopic examination of quartz from the upper impactite interval of the International Continental Scientific Drilling Program (ICDP) Lake Bosumtwi crater drill core LB-07A demonstrates widespread but heterogeneous evidence of shock metamorphism. In the upper impactite, which comprises interbedded polymict lithic breccia and suevite from a drilling depth of 333.4–415.7 m, quartz occurs as a major component within metasedimentary lithic clasts and as abundant, isolated, single-crystal grains within matrix. The noted quartz shock-metamorphic features include phenomena related to a) deformation, such as abundant planar microstructures, grain mosaicism, and reduced birefringence; b) phase transformations, such as rare diaplectic quartz glass and very rare coesite; c) melting, such as isolated, colorless to dark, glassy and devitrified vesicular melt grains; and d) secondary, post-shock features such as abundant, variable decoration of planar microstructures and patchy grain toasting. Common to abundant planar deformation features (PDFs) in quartz are dominated by $\omega\{10\bar{1}3\}$-equivalent crystallographic planes, although significant percentages of $\pi\{10\bar{1}2\}$ and other higher index orientations also occur; notably, *c*(0001) planes are rare. Significantly, the quartz PDF orientations match most closely those reported elsewhere from strongly shocked, crystalline-target impactites. Barometry estimates based on quartz alteration in the upper impactite indicate that shock pressures in excess of 20 GPa were widely reached; pressures exceeding 40–45 GPa were more rare. The relatively high abundances of decorated planar microstructures and grain toasting in shocked quartz, together with the nature and distribution of melt within suevite, suggest a water- or volatile-rich target for the Bosumtwi impact event.

INTRODUCTION

The Bosumtwi impact crater, located in the Ashanti Province, southern Ghana (Fig. 1), is considered to be the youngest well-preserved complex impact structure on Earth. The 1.07 Ma crater has a rim-to-rim diameter of about 10.5 km and is now filled by Lake Bosumtwi, which is approximately 8.5 km in diameter and 80 m deep (Fig. 2). Early work describing the formation of the Bosumtwi structure proposed both cryptoexplosive (Rohleder 1936; Junner 1937) and meteorite impact (MacLaren 1931) mechanisms for its origin. A large body of subsequent geological, geophysical, and geochemical work has clearly demonstrated its impact origin (e.g., Littler et al. 1961; El Goresy 1966; Lippolt and Wasserburg 1966; Schnetzler et al. 1966, 1967; Kolbe et al. 1967; Chao 1968; Jones et al. 1981; Jones 1985a, 1985b; Koeberl et al. 1998; Reimold et al. 1998; Plado et al. 2000; Boamah and Koeberl 2002, 2003, 2006; Scholz et al. 2002; Wagner et al. 2002; Pesonen et al. 2003; Artemieva et al. 2004; Dai et al. 2005; multiple sources in this issue).

This work has also confirmed the hypothesis that the Bosumtwi impact event was the source of the Ivory Coast tektite strewn field (Fig. 1) (Barnes 1961; Lippolt and Wasserburg 1966; Schnetzler et al. 1966, 1967; Glass 1969; Durrani and Khan 1971; Glass and Zwart 1979; Jones 1985a; Koeberl et al. 1996a, 1997, 1998; Dai et al. 2005). Remote sensing, geophysical, and drill core studies demonstrate that the Bosumtwi crater, which is buried beneath up to 294 m of post-impact lacustrine sediments, is a complex impact structure characterized by an annular moat filled with over 135 m of lithic and suevitic impact breccia and by a 130 m high, 1.9 km wide, faulted central uplift overlain by about 25 m of melt-bearing impact-related units (Fig. 2) (Plado et al. 2000; Karp et al. 2002; Scholz et al. 2002; Wagner et al. 2002; Pesonen et al. 2003; Koeberl et al. 2005; Milkereit et al. 2006; multiple sources in this issue).

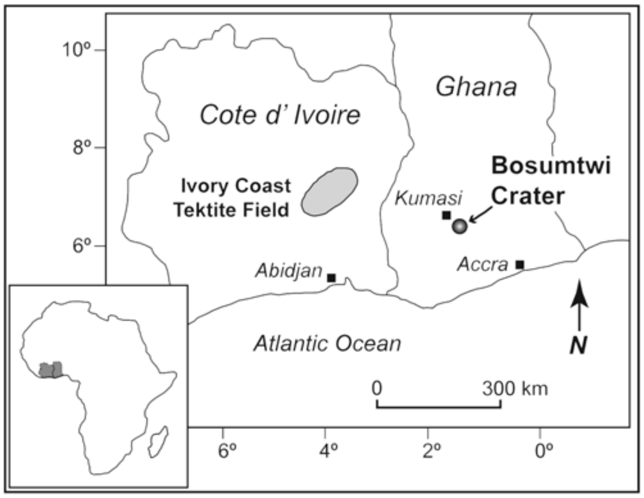

Fig. 1. Generalized locality map of Bosumtwi impact crater, Ghana, and its relation to the Ivory Coast tektite strewn field. Modified from Koeberl et al. (1998) and Koeberl and Reimold (2005).

From July to October, 2004, the Lake Bosumtwi crater was the subject of a multi-national interdisciplinary drilling project led by the International Continental Scientific Drilling Program (ICDP), with financial and logistical support supplied by multiple sources, including Ghana, Austria, the United States, Canada, and South Africa. Using the portable GLAD-800 lake drilling system contracted through DOSECC, Inc. (www.dosecc.org), this collaborative effort yielded 14 drill cores at five sites, which penetrated the 294 m thick, post-impact lake sediment sequence. Two additional hard-rock drill cores, LB-07A and LB-08A, were recovered from crater-filling and crater-floor sequences in the annual moat and over the central uplift, respectively (Fig. 2) (Koeberl et al. 2006a, 2007a).

The primary goals of the 2004 Lake Bosumtwi drilling project were to a) recover a nearly complete, 1-million-year-long, post-impact lake sediment record for reconstructing lake eustatic, sedimentation, and paleoenvironmental histories, and b) obtain critical new subsurface data on the structure, impactite sequences, and crater evolution of this exceptionally well-preserved impact structure. As part of the collaborative effort to meet the second project goal listed above, the purpose of this study is to provide initial observations on the shock-metamorphic alteration of quartz within the upper impactite sequence of drill core LB-07A, recovered from the annular moat of the crater. These observations include the occurrence and general petrographic properties of shocked quartz within the sequence, the abundance and crystallographic orientations of planar microstructures in quartz based on universal stage (U-stage) microscopic examination, and the preliminary results from microRaman spectroscopic analysis of quartz.

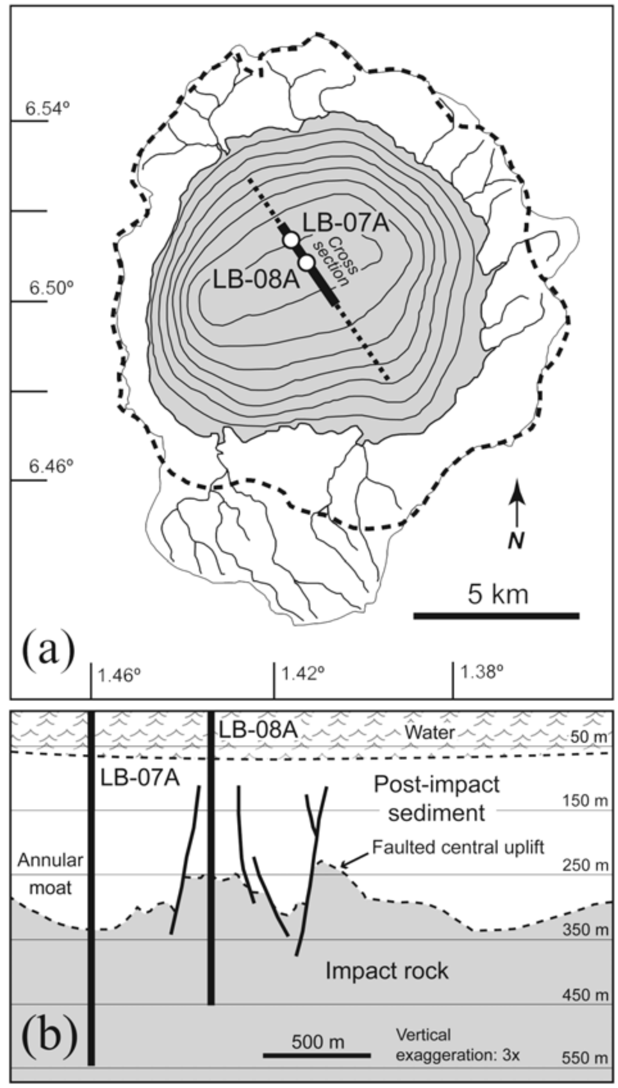

Fig. 2. a) Schematic map of Lake Bosumtwi, Ghana, showing lake drainage basin, lake bathymetry, present morphologic rim of the Bosumtwi impact crater (heavy dashed line), and location of ICDP deep drill cores LB-07A and LB-08A along seismic profile B2000-1, shown by thin dashed line across lake. The bathymetric contour interval is 10 m. b) Generalized interpreted geologic cross-section (heavy solid line at lake center, Fig. 2a) along seismic profile B2000-1, showing units penetrated by drill cores LB-07A and LB-08A. Modified from Jones et al. (1981), Scholz et al. (2002), Koeberl and Reimold (2005), and Milkereit et al. (2006).

Geologic Setting and Stratigraphy of Drill Core LB-07A

Regional geologic units beneath and adjacent to the Bosumtwi crater include lower greenschist facies metamorphic rocks of the 2.097–2.25 Ga Tarkwaian and Birimian Supergroups and a variety of younger Proterozoic felsic, intermediate, and mafic intrusive units (Table 1) (Junner 1937; Woodfield 1966; Moon and Mason 1967; Jones et al. 1981; Reimold et al. 1998; Koeberl and Reimold 2005;

Table 1. Summary of pre-impact geological units, Bosumtwi crater area (after Koeberl and Reimold 2005; Feybesse et al. 2006).

Supracrustal units
Tarkwaian Supergroup (Proterozoic, 2.097–2.13 Ga)
Banket Member quartzite and Kawere Conglomerate
Birimian Supergroup (Proterozoic, 2.1–2.25 Ga)
Metavolcanic rocks (including metasedimentary rocks and altered intrusive rocks, basalt, and spilitic basalt)
Metasedimentary rocks (including meta-graywacke, schist, phyllite, slate, shale, and meta-tuff)
Intrusive units (Proterozoic, 1.98–2.13 Ga)
Basin type
Biotite muscovite granodiorite of Kumasi batholith
Biotite granite and hornblende-biotite granodiorite of Pepiakese granite
Belt type
Biotite granodiorite of Bansu intrusion
Biotite granodiorite of Trobokro sill
Microgranite and quartz porphyry
Minor intrusive rocks
Olivine pyroxenite, dolerite, and gabbro
Amphibolite, pyroxenite, and epidiorite
Granitic dikes associated with Kumasi batholith
Carbonate-rich intermediate dikes

Feybesse et al. 2006; Karikari et al. 2007). Although studies of impactite units within (e.g., Coney et al. 2006, 2007; Ferrière et al. 2006, 2007; Reimold et al. 2006) and outside (Koeberl et al. 1998; Boamah and Koeberl 2003, 2006; Karikari et al. 2007) the crater document a primary contribution from Birimian and (to a lesser extent) Tarkwaian target rocks, a component of rare granitic and other intrusive-igneous clasts within the impactites testify to a probable contribution from the other geologic units as well.

Drill core LB-07A, composed of allochthonous crater-filling impactite and semi-autochthonous crater-floor units, was recovered from a drilling depth of 333.4–545.1 m below lake level (Figs. 2 and 3). Core recovery averaged about 65%, with a range of 10–100% within specific intervals. In general, the highest recovery occurred in the upper half of the cored interval; in the lower half, the core was strongly fractured, commonly disaggregating into smaller fragments or disks. Coney et al. (2007) provide a detailed macroscopic and microscopic description of the LB-07A drill core and divide the core into three informal stratigraphic units—an upper impactite unit, from a depth of 333.4–415.7 m, a lower impactite unit, from a depth of 415.7–470.6 m, and a basement unit, from 470.6 m to the total drilling depth of 545.1 m (Fig. 3).

The basement unit includes dark gray to white metasedimentary megablocks comprising shock-altered shale, graphitic shale, and meta-graywacke. Within the unit, at least two suevitic intercalations, 1 m or less in thickness, were logged, together with one 0.3 m thick layer displaying an unusual granophyre-like texture (Fig. 3). Given the compositional homogeneity of the megablocks and the low abundance of suevite in this interval, this sequence is interpreted as crater floor (Coney et al. 2007). The overlying lower impactite unit is composed of monomict lithic breccia with clasts primarily of meta-graywacke and minor shale, cross-cut by two decimeter-scale suevitic intercalations (Fig. 3).

The upper impactite unit, the focus of this study, comprises two interbedded lithologies of matrix- and clast-supported polymict lithic breccia and of suevitic breccia, present in approximately equal volume percent (Fig. 3) (Coney et al. 2007). In general, polymict lithic breccia is more abundant in the upper half of the upper impactite. The suevite is distinguished from the polymict lithic breccia by a melt component. Upper impactite lithic clasts, which range in average diameter from about 0.1 mm to greater than 2 cm, include, in decreasing abundance, meta-graywacke, phyllite, mica schist, quartzite, shale, and granite. Single-mineral grains, generally 50 μm to 1.0 mm in diameter, include, in decreasing abundance, orthoclase and plagioclase feldspars, quartz, phyllosilicates (biotite, chlorite, and muscovite), carbonate minerals, opaque minerals, and amphibole. In agreement with Coney et al. (2007), no systematic change in mean grain size through the upper impactite unit was noted. The matrix, considered to be particles less than approximately 50 μm across, comprises finely comminuted lithic or mineral grains, clays, and, in suevite, dark melt material. In the upper impactite, matrix makes up approximately 40–75% by volume of the unit (Coney et al. 2007).

The upper impactite suevite includes approximately 2–7% by volume of melt (Table 2 of Coney et al. 2007). The melt occurs as individual particles, often rounded, and as material dispersed in matrix. This melt abundance is comparable to the 6% by volume measured in suevite from

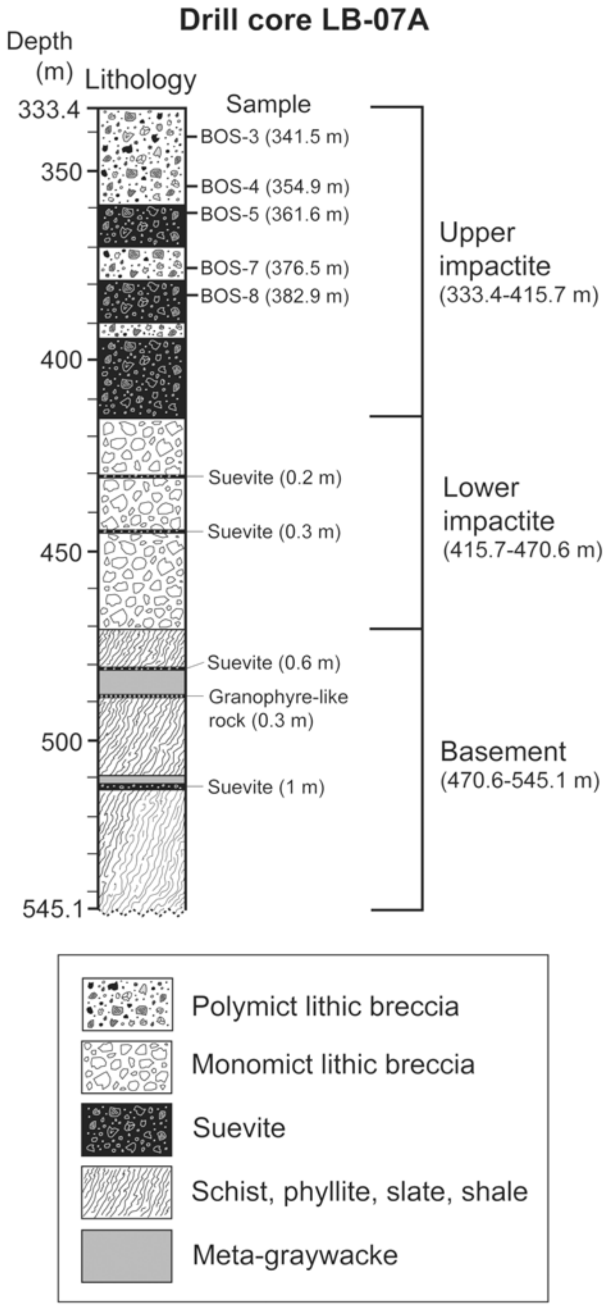

Fig. 3. Generalized stratigraphic column of impact-related units beneath lake sediments, drill core LB-07A, annular moat of Bosumtwi crater. The sequence is divided into upper impactite (333.4–415.7 m), lower impactite (415.7–470.6 m), and basement (470.6–545.1 m) units. Sample numbers and depths below lake level are shown. Modified from Coney et al. 2007.

drill core LB-08A (Ferrière et al. 2007), but significantly less than the 20% by volume reported from suevite outcrops outside of the crater (Boamah and Koeberl 2006). The melt particles occur as both glassy and devitrified grains and sometimes contain other mineral clasts or inclusions within them (Koeberl and Boamah 2006; Coney et al. 2007).

METHODS AND RESULTS

Methods

A total of 10 petrographic thin sections from the LB-07A upper impactite interval were initially evaluated for potential analysis of shocked quartz composition. Among these sections, five were chosen for detailed point-count, U-stage petrographic, and microRaman spectroscopic analyses (Fig. 3), based on the presence of the most abundant shock-metamorphosed quartz. Of these five samples, three are from polymict lithic breccia (BOS-3, 341.5 m depth; BOS-4, 354.9 m depth; BOS-7, 376.5 m depth) and two are from suevite (BOS-5, 361.6 m depth; BOS-8, 382.9 m depth). A five-axis U-stage was used to analyze the crystallographic orientations of 404 sets of planar microstructures in 215 quartz grains, following the measurement and indexing techniques outlined in Engelhardt and Bertsch (1969), Stöffler and Langenhorst (1994), Grieve et al. (1996), and Langenhorst (2002).

Raman spectra were collected with a Renishaw RM1000 confocal edge filter-based microRaman system in the spectral range from approximately 70 cm^{-1} (cut-off of the dielectric edge filters) to 1500 cm^{-1}. The 514.5 nm excitation line of a 40 mW (total) argon ion laser was focused with a 50×/0.75 objective on the polished thin section surface. The back-scattered radiation (180° configuration) was analyzed with a 1200 lines/mm grating monochromator in the “static grating scan” data collection mode. Raman intensities were collected with a thermoelectrically cooled CCD array detector. The resolution of the system (“apparatus function”) with the 514.5 nm line was 4.5 cm^{-1} and the wavenumber accuracy was better than ±1 cm^{-1} (both calibrated with the Rayleigh line and the 520.5 cm^{-1} line of a silicon standard). Spatial resolution was constrained in pseudoconfocal mode to approximately 3 µm both in lateral width and depth. Instrument control and data acquisition were done with Grams/32 software (Thermo Galactic Corporation). Depending on the signal intensity, initial accumulations from 30 to 120 s per “spectral window,” i.e., exposure time of the detector, were measured to identify coesite and other mineral phases. The smooth spectrum of coesite presented herein was obtained with a 30 min long exposure time. Small, highly refractive inclusions in a total of 30 shocked quartz grains from both polymict lithic breccia and suevite were examined; of these inclusions, coesite was positively identified in only one diaplectic quartz grain within the suevite sample BOS-8.

Occurrence of Shocked Quartz

In the upper impactite interval of LB-07A, quartz occurs as single-crystal and polycrystalline constituents within lithic breccia clasts and as single-crystal grains within breccia matrix (Fig. 4). Within the lithic clast population, quartz is the dominant component of quartzite (Fig. 4a) and a common component of meta-graywacke, phyllite, mica schist, and granite (Fig. 4b). Of the lithic grains examined, quartzite clasts are more abundant within polymict lithic breccia in the upper part of interval; these clasts contain the highest percentage of shocked quartz grains, especially grains containing 2 or more sets of planar microstructures (Fig. 4a). Meta-graywacke clasts, comprising up to 42% by volume of the upper impactite interval (Coney et al. 2007), also contain common shocked quartz, although not in the same abundance as noted in quartzite. As is characteristic of the Bosumtwi impact breccias (e.g., Boamah and Koeberl 2003, 2006; Koeberl and Reimold 2005; multiple sources, this issue) and of many other previously described impactite sequences (e.g., French 1998; Koeberl 2001), there is a very heterogeneous distribution of shock levels, both macroscopically and microscopically, within co-occurring lithic and mineral grains in any given interval.

Based on petrographic point-count examination of minerals within lithic clasts and of isolated single-mineral grains in matrix, quartz comprises an overall estimated 10–20% by volume of the mineral constituents. The abundance of quartz showing shock-metamorphic alteration varies from a high value of 61% by volume in sample BOS-3 to a low value of 9% by volume in sample BOS-8 (Table 2). Herein, shock-metamorphic indicators used in estimating the ratio of shocked to unshocked quartz grains include the presence of decorated and nondecorated planar microstructures, optical mosaicism, grain toasting, reduced birefringence, and diaplectic quartz glass (cf. Stöffler and Langenhorst 1994; Grieve et al. 1996; Short and Gold 1996; Langenhorst and Deutsch 1998; Langenhorst 2002; Whitehead et al. 2002). The ratios of shocked to unshocked quartz grains shown in Table 2 probably represent minimum values, as additional shocked quartz grains containing relatively nondecorated planar microstructures (which are not visible under horizontal point-count stage examination) were found subsequently during U-stage analysis.

The most abundant shocked quartz, 61% by volume, was found in polymict lithic breccia of the highest sample, BOS-3, at a depth of 341.5 m (Table 2). This high abundance is significantly greater than that noted in the other, lower samples of both polymict lithic breccia and suevite, which had compositions ranging from 7–20% by volume of shocked quartz. These observations are consistent with the results of Coney et al. (2007, their Table 3), who document 51.4% shock-altered quartz in their highest sample of polymict lithic breccia, at a depth of 334.9 m, with markedly less shocked quartz, ranging from 2.8–22.1%, in samples below.

Planar deformation features (PDFs), which are planar microstructures diagnostic of shock metamorphism (e.g., McIntyre 1962; French and Short 1968; Alexopoulos et al. 1988; Stöffler and Langenhorst 1994; Grieve et al. 1996; Langenhorst 2002), are common to abundant in quartz from polymict lithic breccia and suevite of the Bosumtwi impact event (Chao 1968; Koeberl et al. 1998; Boamah and Koeberl 2003, 2006; Koeberl and Reimold 2005; Coney et al. 2006, 2007; Ferrière et al. 2006, 2007; Morrow 2006). The PDFs are composed of narrow, individual planar elements that are less than 2 μm thick, comprising straight, parallel sets that are spaced 2–10 μm apart. Sample BOS-3 contains 35% by volume of quartz grains with PDFs; quartz in underlying samples contains 2–11% by volume of these planar microstructures (Table 2). Approximately 17–40% of the PDFs are strongly annealed and decorated with tiny, rare to

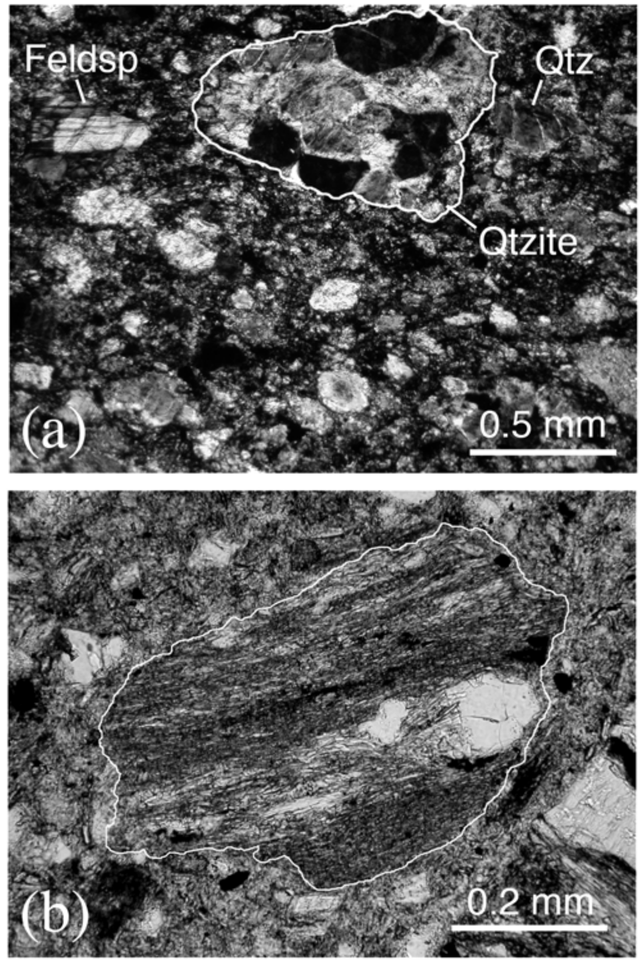

Fig. 4. Thin section photomicrographs showing selected occurrences of quartz within upper impactite unit drill core LB-07A. a) Matrix- to clast-supported polymict lithic breccia, comprising heterolithic, very poorly sorted clasts of single-mineral and lithic grains in a dark matrix dominated by clays and finely comminuted lithic material. Indicated are a relatively large, polycrystalline shocked quartzite clast (Qtzite, circled); a shocked, single-crystal quartz grain (Qtz); and a plagioclase feldspar grain (Feldsp) with kink bands. Sample BOS-3, polymict lithic breccia, cross-polarized light. b) Meta-graywacke to phyllite clast (circled) containing two relatively large, unshocked, single-crystal quartz grains. Sample BOS-5, suevite, plane-polarized light.

Table 2. Petrographic point-count summary of quartz grain properties in upper impactite unit, drill core LB-07A, Bosumtwi crater.

	Polymict lithic breccia			Suevite	
Sample	BOS-3	BOS-4	BOS-7	BOS-5	BOS-8
Depth (m)	341.5	354.9	376.5	361.6	382.9
Grains counted	200	180	109	154	123
	vol% relative to total quartz population within sample				
Unshocked	39	85	93	80	91
Shocked	61	15	7	20	9
PDFs					
Nondecorated	21	5	1.5	8	2.5
Decorated	14	2	0.5	3	0.5
PFs	34	8	3	10	7
Grain mosaicism	40	10	1	14	2
Toasted	41	9	2	15	3
Diaplectic quartz	<1	<1	<1	1	2

abundant vugs or fluid inclusions, discussed below (Table 2) (cf. Robertson et al. 1968; Engelhardt and Bertsch 1969; French 1969; Stöffler and Langenhorst 1994; Grieve et al. 1996). Although beyond the scope of this report, rare PDFs in orthoclase and plagioclase feldspars from both polymict lithic breccia and suevite were also noted.

Other indices of shock metamorphism in quartz, including planar fractures (PFs), optical mosaicism, grain toasting, and reduced birefringence, are also significantly more common in sample BOS-3, following the same abundance trends down-core as noted for the PDF occurrences (Table 2). Diaplectic quartz (Engelhardt et al. 1967; Stöffler 1984; Stöffler and Langenhorst 1994) is present but rare in polymict lithic breccia, comprising less than 1% by volume of the samples; in suevite it is slightly more abundant, reaching about 2% by volume (Table 2). As verified by microRaman analysis, coesite occurs very rarely within diaplectic quartz grains in the suevite.

Properties of Shocked Quartz

Based on classification schemes proposed by Stöffler and Langenhorst (1994), Grieve et al. (1996), Langenhorst and Deutsch (1998), and Langenhorst (2002), the shock-metamorphic properties and processes evident in quartz of the LB-07A upper impactite interval are documented in terms of a) deformation, b) phase transformation, c) melting, and d) secondary, post-shock features. Such phenomena described below are limited to those discernible using standard and U-stage optical petrographic techniques and microRaman spectroscopic analysis.

Deformation

Planar microstructures, comprising PDFs and PFs, constitute one of the most important optical indicators of shock metamorphism in quartz. Examination of upper-impactite shocked quartz under the U-stage microscope documents that the average abundances of PDF sets are 2.0 sets per grain in polymict lithic breccia and 1.6 sets per grain in suevite (Table 3; Fig. 5). This indicates that shocked quartz grains in the polymict lithic breccia contain a higher relative proportion of multiple PDFs sets than grains in the suevite, although the crystallographic orientations of sets in these two lithologies are not significantly different, as discussed below. In both lithic breccia and suevite, 1–2 sets of PDFs are numerically dominant, comprising 77% and 92% by volume, respectively, of the set populations. A maximum of 4 sets per grain are observed; however, where multiple sets are present, they are typically overlapping, are usually moderately to highly decorated, and are sometimes obscured by grain toasting, making it difficult to resolve them optically. Therefore, given this observation and the inherent "blind circle" of the U-stage where planar microstructures cannot be observed (Engelhardt and Bertsch 1969), it is possible that more than 4 sets are present in some grains, which is consistent with petrographic observations of shocked quartz in suevite outside of the crater (Boamah and Koeberl 2006).

Individual PDF sets may cross the entire quartz crystal (Figs. 6a and 6b) or, more commonly, are apparently concentrated within the grain interiors (Fig. 6c). Where sets do not reach the grain margins, evidence of annealing in the form of microscopic vugs or fluid inclusions, which may document the prior existence of PDFs, is rare (cf. Fig. 6c). Many of the shocked grains are composed of polycrystalline, or multiple-domain, quartz (Figs. 6d, 6e, and 6f). Within polycrystalline quartz clasts, the number and orientations of PDF sets between individual domains usually vary, attesting to the small-scale, heterogeneous distribution of shock energy within and between the grains.

The PDFs are dominated by planes with $\omega\{10\bar{1}3\}$-equivalent crystallographic orientations, which comprise approximately 50% of the indexed PDF sets in both polymict lithic breccia and suevite quartz grains (Table 3; Fig. 5).

Table 3. Summary of PDF set abundance and indexed PDF crystallographic orientations in quartz within upper impactite unit, drill core LB-07A, Bosumtwi crater.

	Polymict lithic breccia	Suevite	Combined
No. of sets	305	99	404
No. of grains	154	61	215
No. of PDF sets/grain	305/154 = 2.0	99/61 = 1.6	404/215 = 1.9
PDF sets; relative % of shocked quartz grains examined			
1 set	31	49	36
2 sets	46	43	45
3 sets	18	5	14
4 sets	5	3	5
Total	100	100	100
Indexed PDF orientations; absolute frequency (%)[a]			
Form			
c(0001)	3	6	4
$\omega\{10\bar{1}3\}$	54	48	52
$\pi\{10\bar{1}2\}$	15	18	16
$r/z\{10\bar{1}1\}$	5.5	6	5.5
$m\{10\bar{1}0\}$	1.5	2	1
$\xi\{11\bar{2}2\}$	2	2	2.5
$s\{11\bar{2}1\}$	4	5	4
$a\{11\bar{2}0\}$	1	1	1
$\{22\bar{4}1\}$	n.d.	1	0.5
$x\{51\bar{6}1\}$	2	1	2
$\rho\{21\bar{3}1\}$	5	7	5.5
Unindexed	7	3	6
Total	100	100	100

[a]Method described in Engelhardt and Bertsch (1969), Stöffler and Langenhorst (1994), Grieve et al. (1996), and Langenhorst (2002).
n.d. = none detected.

Planes with $\pi\{10\bar{1}2\}$ orientations are also common, comprising 15–18% of PDF sets in lithic breccia and suevite samples, respectively. In decreasing abundance, other measured PDF set orientations include $\rho\{21\bar{3}1\}$, $r/z\{10\bar{1}1\}$, $s\{11\bar{2}1\}$, c(0001), $\xi\{11\bar{2}2\}$, $m\{10\bar{1}0\}$, $x\{51\bar{6}1\}$, $a\{11\bar{2}0\}$, and $\{22\bar{4}1\}$. In terms of crystallographic orientations and absolute percentages of PDF sets, there does not seem to be a significant difference between quartz in the polymict lithic breccia and suevite.

Planar fractures are another important microstructure type within the quartz (Table 2), occurring in up to 34% by volume of the grain populations. The PFs occur as parallel sets of open and closed planes, which are generally greater than 3 µm thick and spaced greater than 10 µm apart. Within the LB-07A samples, the majority of measured PFs show $r/z\{10\bar{1}1\}$ orientations, although planes parallel to c(0001) and, more rarely, $\omega\{10\bar{1}3\}$ are also present. Where $\omega\{10\bar{1}3\}$ planes occur, they are sometimes transitional to, and parallel with, similarly oriented PDF sets (Fig. 7a) (cf. Stöffler and Langenhorst 1994).

As documented previously in shocked quartz from other impact structures, PFs often control and limit the distribution of adjacent PDF sets, evidencing that PF formation predated PDF formation within the crystal (Fig. 7b) (cf. Engelhardt and Bertsch 1969; Stöffler and Langenhorst 1994; French et al. 1997, 2004; French 1998). In several cases within the Bosumtwi quartz grains, incipient PDF sets appear to radiate from earlier-formed PFs and curviplanar cleavage fractures, producing a distinctive "feather texture," which may evidence sites in the crystal that received shock energy at the threshold of PDF development, about 10 GPa (Stöffler and Langenhorst 1994; French et al. 2004; Morrow 2006).

Grain mosaicism comprises a second important deformation phenomenon within shocked quartz of the upper impactite interval. Up to 40% by volume of the quartz grains show some effects of mosaicism, which is characterized by an irregular or mottled optical extinction pattern, with the crystal containing many smaller subdomains that range downward in size to the limit of petrographic resolution (Fig. 8) (Stöffler and Langenhorst 1994). Mosaicism is most common and well developed in grains containing such other evidence of shock metamorphism as planar microstructures and toasting. Because of the relatively wide scatter of optic axes in different subdomains of mosaic quartz crystals, it is possible to document the relative degree of mosaicism with the U-stage microscope by measuring and comparing the optic axis dispersal polygon areas of multiple grains relative to the total area of a Schmidt equal-area net (Fig. 9) (Dachille et al. 1968). Mosaic quartz grains from the upper impactite interval in LB-07A plot clearly within the region expected for shocked quartz (Fig. 9). A third effect of shock deformation in quartz is reduced birefringence (Stöffler and Langenhorst

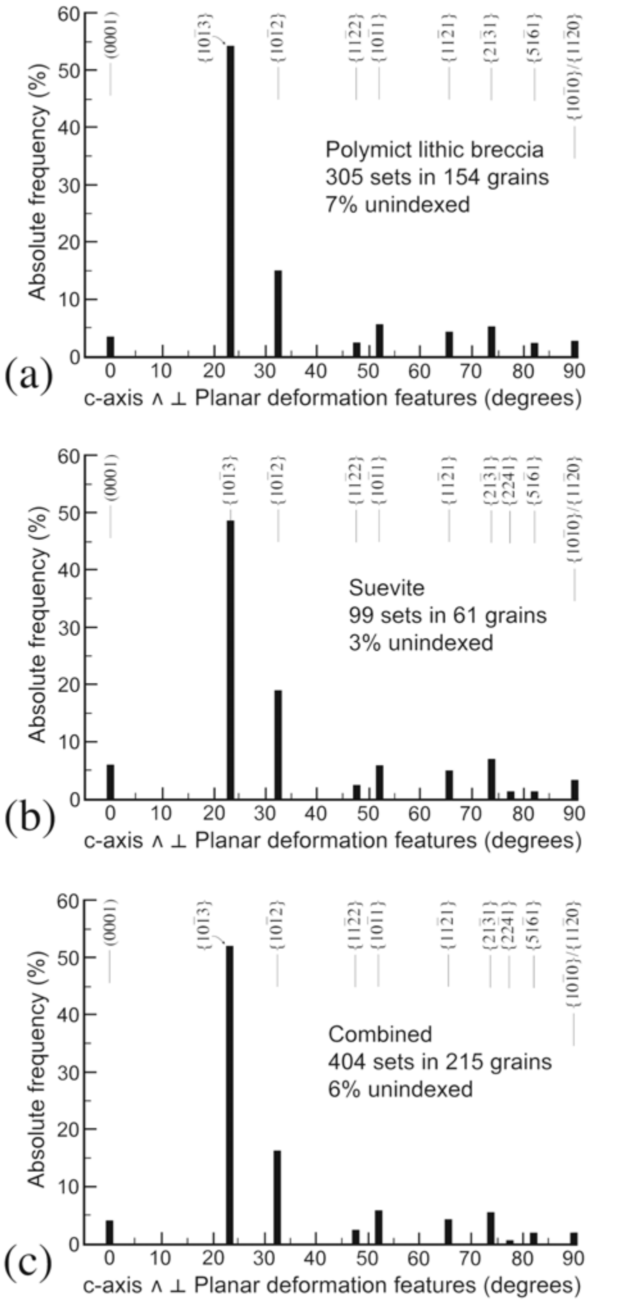

Fig. 5. Histograms of absolute frequency percent of indexed PDFs in quartz, upper impactite unit drill core LB-07A. a) Plot of PDFs in quartz from polymict lithic breccia, samples BOS-3, BOS-4, and BOS-7. b) Plot of PDFs in quartz from suevite, samples BOS-5 and BOS-8. c) Plot of combined PDF data from both polymict lithic breccia and suevite. Indexing method after Engelhardt and Bertsch (1969), Stöffler and Langenhorst (1994), Grieve et al. (1996), and Langenhorst (2002).

1994; Grieve et al. 1996), which is identified qualitatively in this study on the basis of maximum first-order interference color variability in thin section, with consideration given to individual grain orientations and changes in section thickness.

Phase Transformations

The primary phase transformation features evident in optical and microRaman spectroscopic examination of the upper impactite quartz are rare diaplectic quartz glass and very rare examples of the high-pressure SiO_2 polymorph coesite (French and Short 1968; Stöffler 1972, 1984; Stöffler and Langenhorst 1994; Grieve et al. 1996). Diaplectic quartz is present both in polymict lithic breccia and in suevite, comprising less than 1% and 1–2% by volume, respectively (Table 2). In general, the diaplectic quartz is characterized by isotropic extinction patterns, abundant tiny vugs and fluid inclusions, grain toasting, and decorated and nondecorated PDFs (Fig. 10). Based on these limited occurrences, it appears that the diaplectic quartz is slightly more common within the suevite. Rare maskelynite, diaplectic feldspar glass, was also observed in both the polymict lithic breccia and suevite and, as in the case of diaplectic quartz, it appears slightly more common within suevitic samples.

Littler et al. (1961) reported the occurrence of coesite, based on XRD analysis, from a surface outcrop of suevite near the Bosumtwi crater rim. Within the LB-07A upper impactite interval, coesite is now documented within a diaplectic quartz grain occurring in suevite sample BOS-8 (Fig. 11). The coesite occurs with quartz as highly refractive, light green grains and beaded aggregates (cf. Stöffler 1971a; French 1998) less than 50 µm across that are concentrated near and adjacent to probable melt veinlets cross-cutting the diaplectic quartz grain (Fig. 11a). MicroRaman analysis of the coesite yielded diagnostic spectral peaks matching those reported previously from other examples of synthetic and natural coesite (Fig. 11b; Table 4) (Boyer et al. 1985; Ostroumov et al. 2002).

Melting

The preliminary occurrence, distribution, and properties of melt in suevite both within and outside of the Bosumtwi crater are now documented (e.g., Koeberl et al. 1998; Boamah and Koeberl 2003, 2006; Coney et al. 2006, 2007; Ferrière et al. 2006, 2007). Coney et al. (2007) distinguish both mafic melt, comprising 95% of the melt particle population and characterized by dark color under plane-polarized light, flow structures, and rare vesicles, and felsic melt, which comprises 5% of the melt grains and is characterized by colorless to white color under plane-polarized light, flow structures, and common vesicles. As indicated by trace-element analyses, glassy melt of probable quartz-rich composition is present in suevite outside the crater (Koeberl et al. 1998). Similar millimeter-scale melt particles, which appear as isotropic, colorless, glassy, flow-banded, and vesicle-rich grains, are noted within the upper impactite suevite in this study (Fig. 12), indicating the possible occurrence of quartz-rich melt or lechatelierite. In agreement with Coney et al. (2007), no ballen quartz was noted in the LB-07A upper impactite interval, although it is present in suevite outside of the crater (Boamah and Koeberl 2006; Karikari et al. 2007).

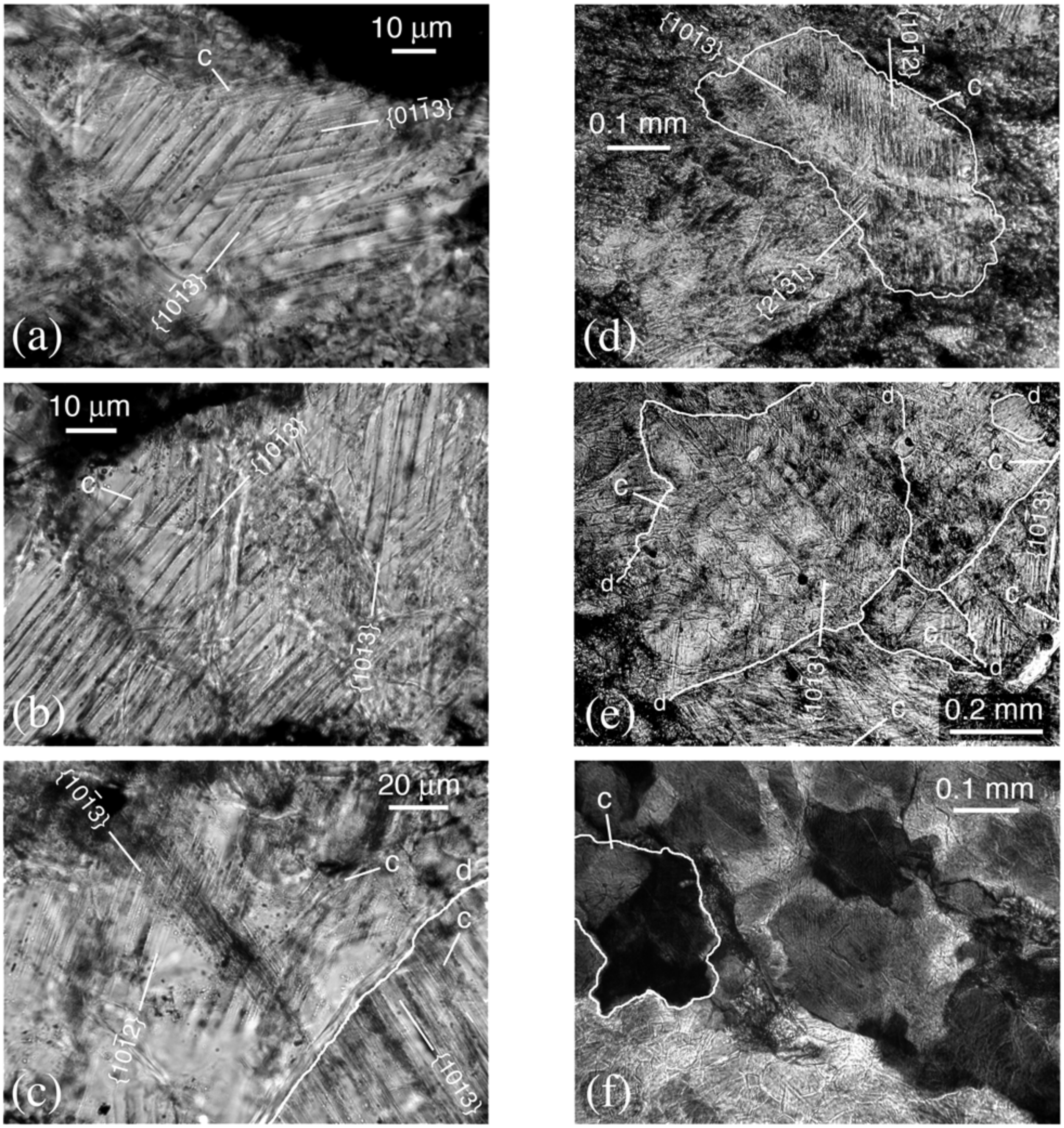

Fig. 6. Thin section photomicrographs of indexed PDFs in shocked quartz, upper impactite unit, drill core LB-07A. a) Grain with two strong, relatively nondecorated PDF sets, $\omega\{10\bar{1}3\}$ and $\omega'\{01\bar{1}3\}$; orientation of quartz c-axis is shown. Sample BOS-3, polymict lithic breccia, plane-polarized light. b) Second grain with two strong, relatively nondecorated PDF sets, both with positive $\omega\{10\bar{1}3\}$-equivalent orientation; quartz c-axis is indicated. Sample BOS-3, polymict lithic breccia, plane-polarized light. c) Grain with two crystallographic domains, indicated by line (d) along the domain boundary. Left crystal contains two partially decorated, intersecting PDF sets, with $\omega\{10\bar{1}3\}$ and $\pi\{10\bar{1}2\}$ orientations. Note development of dark, patchy, inclusion-rich toasted area where PDF sets cross. Right crystal contains one well-developed, partially decorated PDF set with $\omega\{10\bar{1}3\}$ orientation, which terminates against domain boundary. Quartz c-axes are indicated. Sample BOS-3, polymict lithic breccia, plane-polarized light. d) Single domain (circled) within shocked quartzite clast, showing strong $\pi\{10\bar{1}2\}$ and weak $\omega\{10\bar{1}3\}$ and $\rho\{2\bar{1}\bar{3}1\}$ PDF orientations; a fourth weak PDF set, also with probable $\omega\{10\bar{1}3\}$-equivalent orientation, is visible under U-stage rotation. Quartz c-axis is indicated. Sample BOS-3, polymict lithic breccia, plane-polarized light, U-stage view. e) Overview of shocked quartzite clast, showing boundaries between crystallographic domains (labeled "d"), orientations of c-axes within grains, and two prominent $\omega\{10\bar{1}3\}$ PDF sets; other unlabeled PDF sets are visible. Sample BOS-3, plane-polarized light, polymict lithic breccia, U-stage view. f) Second overview of a shocked quartzite clast, showing multiple crystallographic domains, several moderate to strong PDF sets, and one grain (circled, averaged c-axis labeled) with well-developed mosaicism. Sample BOS-5, suevite, cross-polarized light, U-stage view.

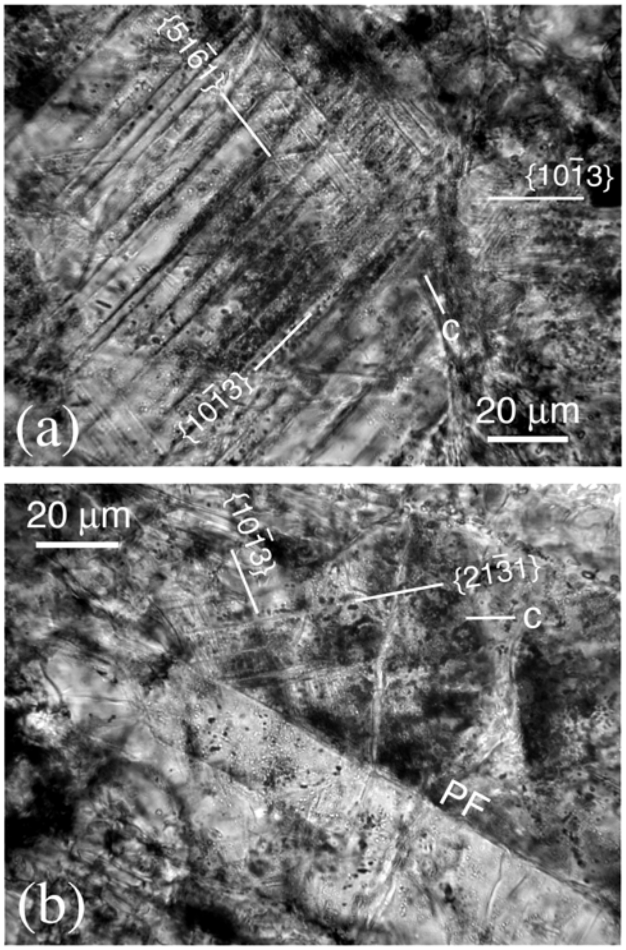

Fig. 7. Thin section photomicrographs of PFs and PDFs in quartz, upper impactite unit, drill core LB-07A. a) Three sets of planar microstructures, including a strong, partially decorated set with $\omega\{10\bar{1}3\}$-equivalent orientation, which includes closed PFs (left) and PDFs (upper right); a second, nondecorated set with $x\{51\bar{6}1\}$ orientation; and a third weak, partially decorated set also with $\omega\{10\bar{1}3\}$ orientation; c-axis is shown. Note patchy toasting in grain center and in upper center portion of view, where $\omega\{10\bar{1}3\}$ and $x\{51\bar{6}1\}$ sets intersect. Sample BOS-3, polymict lithic breccia, plane-polarized light. b) Single-crystal grain cross-cut by one prominent open PF (labeled), separating the relatively unshocked lower-left portion of grain from the highly shocked upper-right portion, which contains at least two sets of decorated planar microstructures ($\omega\{10\bar{1}3\}$ and $\rho\{21\bar{3}1\}$, labeled) and abundant dark, inclusion-rich toasted regions; c-axis is shown. Sample BOS-3, polymict lithic breccia, plane-polarized light.

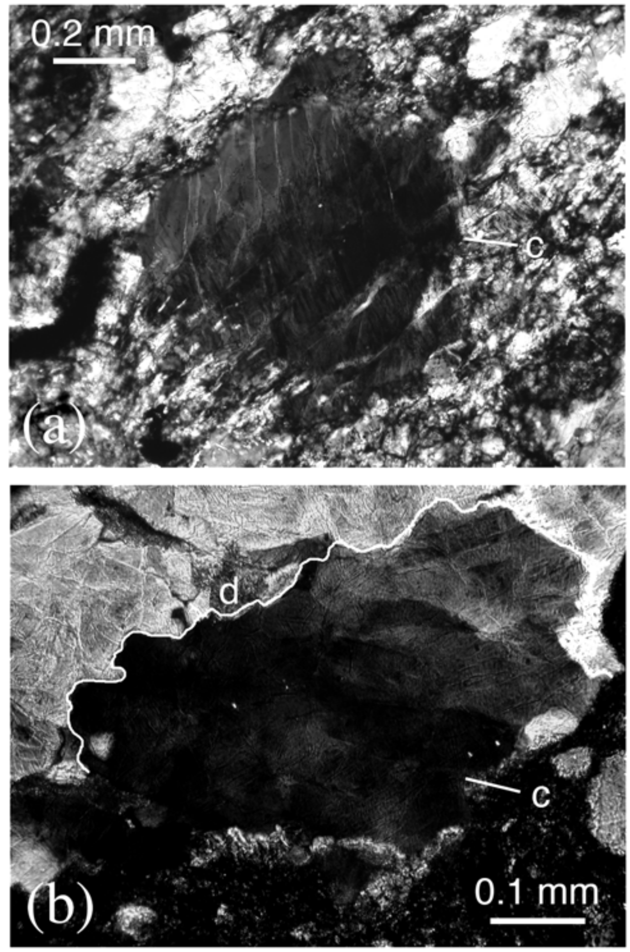

Fig. 8. Thin section photomicrographs with examples of mosaicism in shocked quartz, upper impactite unit, drill core LB-07A. a) Single-crystal grain cross-cut by open, subplanar to curviplanar cleavage fractures, which appear to be concentrated in the grain region showing the strongest development of mosaic fabric; averaged c-axis is indicated. Sample BOS-8, suevite, cross-polarized light. b) Grain within shocked quartzite clast (crystallographic domain boundary indicated by line and "d") showing well-developed mosaicism; averaged c-axis is shown. Sample BOS-5, suevite, cross-polarized light, U-stage view.

Secondary Features

The two most important secondary, post-shock features evident within quartz grains are decoration of planar microstructures and grain toasting. Up to 40% of the PDFs within the upper impactite interval are decorated by rare to abundant vugs or fluid inclusions that are generally less than 2 µm in diameter (Table 2) (cf. Robertson et al. 1968; Engelhardt and Bertsch 1969; French 1969; Stöffler and Langenhorst 1994; Grieve et al. 1996). The distribution of decorated PDFs is very localized within the shocked quartz grains, and individual planes and planar sets may be both relatively decorated and nondecorated (Fig. 13). The occurrence and abundance of decorated PDFs are similar to those seen in the PDF distribution itself, i.e., decorated planes are most often concentrated within the grain interiors and commonly do not cross the entire crystal.

Grain toasting (Short and Gold 1996; Whitehead et al. 2002) is also a diagnostic optical property of shocked quartz within the upper impactite interval, occurring in up to 41% by volume of the grains (Table 2). Under plane-polarized light, the toasting appears as heterogeneously distributed, cloudy, dark brown to black, nonpleochroic patches within shocked grains also characterized typically by strong PDF development and, under cross-polarized light, mosaicism and reduced birefringence (Figs. 6c, 7, 10a, and 13). The material

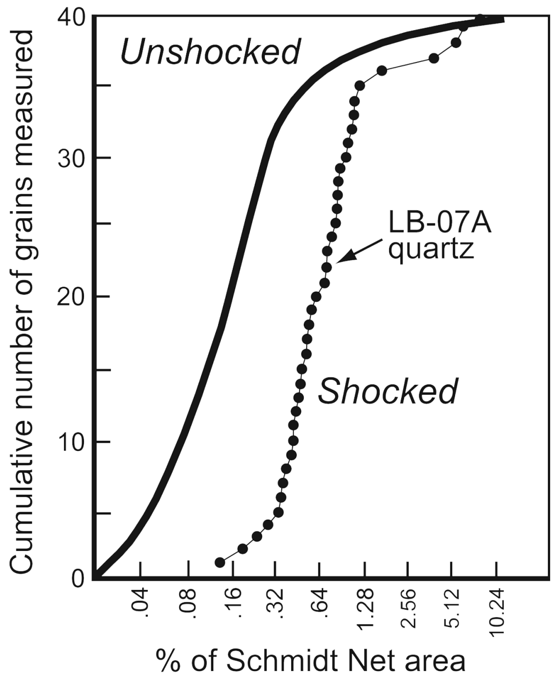

Fig. 9. Plot of the cumulative number of quartz grains with mosaicism in upper impactite interval, LB-07A, whose optic axis dispersal polygon areas are equal to or smaller than the corresponding percentage area of the total Schmidt net, denoted along abscissa. The graph is based on measurement of 135 optic axes in 40 mosaic quartz grains from both polymict lithic breccia and suevite. The heavy curved line, which separates regions of shock and no shock, was empirically derived by comparison of quartz optic axis dispersal polygon areas from seven documented impact sites and eight tectonically dominated, non-impact localities. Modified from Dachille et al. (1968).

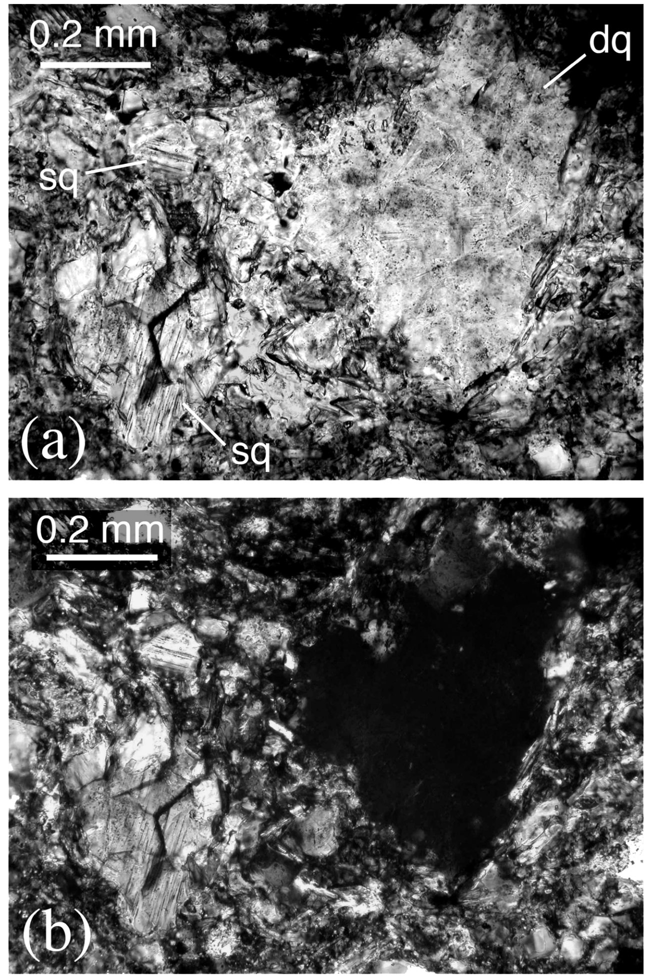

Fig. 10. Thin section photomicrograph of diaplectic quartz in suevite, sample BOS-5, upper impactite unit, drill core LB-07A. a) Plane-polarized light view, showing meta-graywacke clast containing quartz and feldspar, including two small, shocked quartz grains (sq; prominent, partially decorated PDF sets are probably $\omega\{10\bar{1}3\}$) and one larger, shocked diaplectic quartz grain (dq; poorly preserved PDFs, inclusion-rich patches, and minor toasting visible in grain interior). b) Same view under cross-polarized light, showing isotropic extinction pattern of diaplectic quartz grain.

comprising the toasted regions cannot be resolved optically with the petrographic microscope. However, a transmission electron microscope study of toasted quartz (Whitehead et al. 2002) revealed the presence of abundant submicrometer-scale fluid inclusions, probably composed of water exsolved from recrystallized melt glass within adjacent PDF lamellae, which characterize the dark, cloudy regions.

Typically, the toasted patches are best developed where decorated PDF sets also occur and, in some cases, there appears to be a lateral transition from heavily decorated PDFs into the toasted regions (Fig. 13). Toasted patches also seem to be more common where two or more decorated PDF sets, comprised usually of one $\omega\{10\bar{1}3\}$-equivalent set together with one or more higher index set(s), intersect (Figs. 6c, 7, and 13c). In areas where the toasting is especially robust, PDFs can be masked and difficult to discern under the U-stage microscope. As noted for some PDFs, the distribution of grain toasting is spatially associated with and possibly controlled by PFs and cleavage (Figs. 13a and 13b), indicating that toast formation may have been a later feature. This observation, together with the close association of toasted patches with decorated PDFs and abundant micro-inclusions (Whitehead et al. 2002), supports the hypothesis that toasting is a feature intimately tied to PDF development, post-shock annealing, and fluid exsolution.

DISCUSSION

Comparison with Other Bosumtwi Studies

The observations of upper impactite shocked quartz presented in this study compare well with other petrologic and petrographic data reported from the LB-07A and LB-08A cores taken within the Bosumtwi crater (Coney et al. 2006, 2007; Ferrière et al. 2006, 2007). As noted by these workers, however, significant differences do exist between the impactites within the LB drill cores and

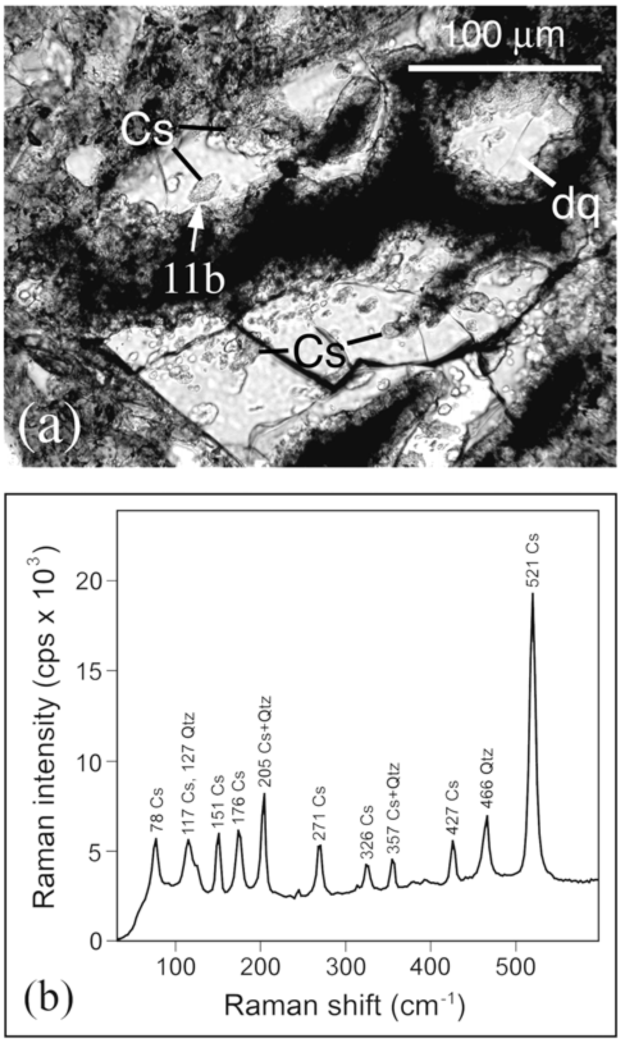

Fig. 11. Coesite in quartz within suevite, upper impactite unit, drill core LB-07A. a) Photomicrograph of grains and beaded aggregates of light green, highly refractive coesite (Cs) within diaplectic quartz clast (dq). Sampling site for Raman spectrum shown in Fig. 11b is indicated. Diaplectic quartz clast is cross-cut by dark brown, cloudy, amorphous veinlets of probable altered melt, which yielded nondiagnostic Raman spectra characterized by high background interference and a lack of recognizable peaks. Sample BOS-8, plane-polarized light. b) Raman spectrum of grain illustrated in Fig. 11a, comprising coesite and quartz. Moderate to very strong diagnostic coesite (Cs), quartz (Qtz), and overlapping coesite and quartz (Cs+Qtz) peaks are labeled (Table 4); Raman intensity indicated along ordinate is in counts per second (cps), an arbitrary value.

impactites analyzed outside of the crater (e.g., Koeberl et al. 1998; Koeberl and Boamah 2003, 2006; Koeberl and Reimold 2005; multiple sources, this issue). These differences are primarily in the amount of melt material and in the level of shock metamorphism evidenced by quartz and other minerals, as recorded by abundances of PDFs, diaplectic quartz glass, and ballen quartz. These parameters together indicate that the maximum shock level experienced by material emplaced in suevitic ejecta outside of the crater is notably higher than for impactites studied thus far inside the crater.

In general, the U-stage data on indexed quartz PDFs presented herein correlate well with similar data sets from suevite in drill core LB-08A (Ferrière et al. 2007) and outside the crater (Boamah and Koeberl 2006). The same crystallographic orientations ($\omega\{10\bar{1}3\}$, $\pi\{10\bar{1}2\}$, etc.) were noted in shocked quartz from all localities. Minor differences are evident, however, between the measurements herein (Table 3; Fig. 5) and 1) LB-08A shocked quartz (Fig. 10 of Ferrière et al. 2007), which displays a lower percentage of $\pi\{10\bar{1}2\}$ planes (less than 5% as compared to 15–18% in LB-07A upper impactites), and 2) shocked quartz outside the crater (Table 3 and Figs. 7 and 8 of Boamah and Koeberl 2006), which contains significantly more $\pi\{10\bar{1}2\}$ planes (32–37% as compared to 15–18% in LB-07A upper impactites) and significantly higher percentages of shocked grains with 2–4 PDF sets per grain (and hence greater PDF plane-to-grain ratios), as well as quartz containing 5 PDF sets per grain, a feature not recorded in LB-07A.

Comparison with Other Impact Structures

The crystallographic orientations and percentage abundances of PDFs documented from the Bosumtwi impactites (Table 3; Fig. 5) (Figs. 7 and 8 of Boamah and Koeberl 2006; Fig. 10 of Ferrière et al. 2007) compare favorably with PDF data sets reported from other crystalline-target impact sites. Most notable in the Bosumtwi shocked quartz is the relatively low abundance or absence of *c*(0001) planes; the relatively high abundance, especially outside of the crater and in the LB-07A upper impactites, of $\pi\{10\bar{1}2\}$ planes; and the occurrence of several relatively low-abundance, higher index plane orientations. Similar PDF distributions are reported from such impact sites as West Clearwater Lake (Engelhardt et al. 1968; indexed and replotted in Grieve et al. 1996), multiple Canadian craters, including also West Clearwater Lake data (both type C and D planar features) (Robertson et al. 1968), Ries (Engelhardt and Bertsch 1969; indexed and replotted in Grieve et al. 1996), North American Cretaceous-Tertiary boundary localities (Bohor et al. 1987; Grieve and Alexopoulos 1988; indexed and replotted in Grieve et al. 1996), Gosses Bluff (Fig. 23 of Grieve et al. 1996), Manson (Short and Gold 1996), and Woodleigh (i.e., lower half of the Woodleigh 1 core, Reimold et al. 2003).

In the case of Gosses Bluff, the measured shocked quartz grains were from a tightly cemented quartz sandstone, which apparently had shock-response properties similar to that of quartz from a typical crystalline target rock (Grieve et al. 1996). As such, the Gosses Bluff example may be a good analog for the Tarkwaian and Birimian metasedimentary units comprising the Bosumtwi target. In

Table 4. Raman peak frequencies (in cm^{-1}) between 75 and 1200 cm^{-1} for coesite (Cs) in quartz (Qtz) from suevite sample BOS-8, upper impactite unit, drill core LB-07A, Bosumtwi crater, compared with other selected spectra.

Peak type	BOS-8	Coesite[b]	Coesite[c]	Coesite + quartz[d]	Quartz[e]
Cs	77.5 (m)[a]	77 (m)	–	–	–
Cs	116.5 (m)	118 (s)	118 (s)	117 (s)	–
Qtz	127 (m)	–	–	127 (s)	127 (s)
Cs	151 (m)	151 (m)	151 (m)	150 (m)	–
Cs	176 (m)	176 (s)	177 (s)	177 (s)	–
Cs + Qtz	204.5 (s)	204 (m)	205 (m)	205 (m)	206 (s)
Cs	244 (vw)	245 (vw)			
Qtz	–	–	–	–	265 (w)
Cs	270.5 (m)	270 (s)	270 (s)	270 (s)	–
Cs	326 (m)	326 (m)	326 (m)	325 (m)	–
Cs + Qtz	356.5 (m)	355 (m)	357 (m)	356 (m)	355 (m)
Cs	380.5 (vw)	381 (vw)	–	–	–
Qtz	394.5 (vw)	–	–	–	394 (m)
Qtz	–	–	–	–	401 (w)
Cs	427 (m)	427 (s)	427 (s)	–	–
Qtz	466 (m)	467 (w)	465 (s)	464 (m)	464 (vs)
Qtz	–	–	–	–	509 (w)
Cs	521 (vs)	521 (vs)	521 (vs)	520 (s)	–
Cs	662 (vw)	662 (vw)	661 (vw)	–	–
Qtz	–	–	–	–	695 (vw)
Cs	786.5 (w)	787 (w)	789 (w)	–	–
Cs	–	–	–	794 (w)	
Qtz	–	–	807 (vw)	804 (w)	806 (w)
Cs	814.5 (w)	815 (vw)	816 (vw)	–	–
Cs	836 (w)	838 (w)	834 (vw)	834 (w)	–
Cs	1039 (w)	1040 (w)	1040 (w)	–	–
Cs + Qtz	1065 (w)	1066 (vw)	1066 (vw)	1064 (w)	1064 (w)
Qtz	–	–	–	1081 (w)	1083 (w)
Cs	1146.5 (w)	1146 (w)	1144 (vw)	–	–
Cs + Qtz	1165 (m)	1165 (w)	1164 (w)	1160 (w)	1162 (w)

[a]Spectral peak strength: vw = very weak; w = weak; m = medium; s = strong; vs = very strong. Approximate measurement accuracy of BOS-8 samples: 2 cm^{-1} for very weak to weak bands, 1 cm^{-1} for medium to very strong bands.
[b]Laboratoire de Sciences de la Terre, ENS-Lyon, France; http://www.ens-lyon.fr/LST/Raman, accessed 19 December 2006.
[c]Kimberlite, sample GRR 1603, Kimberley, South Africa (514.5 nm data); Division of Geological and Planetary Sciences, California Institute of Technology; http://minerals.caltech.edu/files/raman, accessed 19 December 2006.
[d]Chicxulub impactite, sample R79-2, from Ostroumov et al. (2002).
[e]Unshocked quartz, sample BOS-8, this study; analytical methods described herein.

contrast, shocked quartz PDF orientations and abundances from presumably porous sedimentary target-dominated impact sites, e.g., Barringer crater (Carter 1965), B.P. and Oasis structures (French et al. 1974), the Newporte crater (Koeberl and Reimold 1995), the Red Wing crater (Koeberl et al. 1996b), and the Alamo Breccia (Morrow and Sandberg 2001), are not a good match for the Bosumtwi shocked quartz as they contain much more abundant *c*(0001) planes and high-index PDF orientations. Impactites that were sourced from targets containing both crystalline and porous sedimentary rocks, e.g., in the Chesapeake Bay crater (Koeberl et al. 1996a), contain quartz PDF populations that appear intermediate in orientation and abundance between the crystalline (i.e., Bosumtwi) and sedimentary endmembers, evidencing the broad and heterogeneous range of PDF formation expected in mixed-target impact events (Grieve et al. 1996).

Shock Barometry

The wide spectrum of shock-metamorphic indicators in quartz of the upper LB-07A drill core attests to the heterogeneous mixing of variably shocked target materials during the impact event and subsequent emplacement of the impactite sequence. Based on observations of quartz deformation features including the low abundance of *c*(0001) planes and the common occurrences of $\pi\{10\bar{1}2\}$, $r/z\{10\bar{1}1\}$, and $\xi\{11\bar{2}2\}$ PDF orientations, the upper impactite sequence experienced a widespread peak shock-metamorphic pressure of at least 20 GPa (Robertson and Grieve 1977; Stöffler and Langenhorst 1994). This corresponds to shock stages Ia and Ib, derived from experimental data (Stöffler 1971b, 1984), or shock stage 4, strongly shocked, derived from empirical observation of PDF orientations in quartz from impactites (Table 5 of

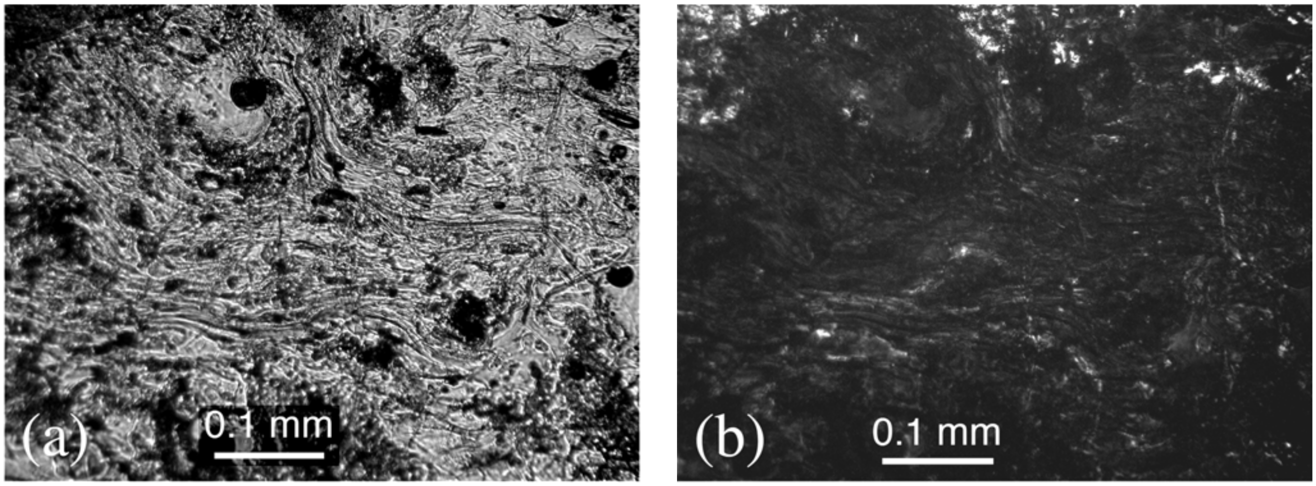

Fig. 12. Thin section photomicrograph of glassy, colorless, vesicular, flow-banded, inclusion-rich melt grain, possibly lechatelierite, sample BOS-8, suevite in upper impactite unit, drill core LB-07A, viewed in (a) plane-polarized and (b) cross-polarized light.

Stöffler and Langenhorst 1994). Such rarer phase transformation features as diaplectic quartz glass and coesite evidence shock pressures greater than approximately 30 GPa, while silicate melt particles indicate that shock pressures in excess of about 45–50 GPa were reached (Stöffler and Langenhorst 1994; French 1998; Langenhorst 2002). This corresponds to shock stages II–III of Stöffler (1971b, 1984).

These observations are consistent with the conclusions of Coney et al. (2007), based on the upper impactite and underlying units of the LB-07A drill core, and with those of Ferrière et al. (2007) from the LB-08A drill core over the central uplift. Shock barometry indicators from suevitic units outside the crater, which include relatively abundant diaplectic quartz glass, ballen quartz, and melt (Koeberl et al. 1998; Boamah and Koeberl 2003, 2006), together with coesite (Littler et al. 1961) and baddeleyite (El Goresy et al. 1968), demonstrate that these impactites experienced relatively widespread maximum shock pressures of at least 50 GPa (Boamah and Koeberl 2006).

Within the upper impactite sequence at LB-07A, the average maximum shock levels increase downcore, as evidenced by the higher percentage of melt and suevite, and slightly higher percentages of diaplectic quartz glass and $\pi\{10\bar{1}2\}$-oriented PDF planes (Tables 2 and 3; Fig. 5) (cf. Coney et al. 2007). An exception to this trend is found in the stratigraphically highest sample, BOS-3, which contains the highest percentage by volume of shocked quartz and the highest average number of PDF sets per grain (Table 2). Furthermore, this interval contains the most quartzite lithic fragments. Based on these observations, the highest portion of the upper impactite interval, i.e., above a drilling depth of about 350 m, may contain a larger component of ballistically transported fallout material that was sourced higher in the target sequence. Elsewhere in the crater, a thin ejecta layer, which contains shocked quartz, accretionary lapilli, and microtektite-like glassy spherules, caps the impactite sequence (Koeberl et al. 2006b, 2007b) and may give further evidence of a significant fallout component at the top of the crater-filling impact sequence.

Target Saturation

One important unanswered question regarding the Bosumtwi impact event is why abundant melt-rich impactites or coherent impact melt sheets did not develop during the event (e.g., Artemieva et al. 2004; Artemieva 2007). The majority of the reported melt occurs as widely disseminated particles or, more rarely, as bombs within suevite (Koeberl et al. 1998; Koeberl and Boamah 2003, 2006; Coney et al. 2007; Ferrière et al. 2007). Modeling by Kieffer and Simonds (1980) and Melosh (1989) suggests that impact into a water- or volatile-rich porous target would not be expected to produce coherent melt bodies but instead would preferentially favor the development of dispersed melt within heterolithic breccias, i.e., suevites, such as seen in and around the Bosumtwi crater. Field observations of marine-target impact structures demonstrate that most, but not all, of these craters are characterized by the lack of coherent melt deposits (Ormö and Lindstrom 2000; Dypvik and Jansa 2003). Furthermore, the relative development of other shock products like diaplectic quartz glass may also be hampered by a saturated target (Masaitis et al. 1991). Therefore, the pre-impact bulk-rock properties of the Bosumtwi target, including porosity, saturation, and competency, together perhaps with the angle of impact (e.g., Deutsch 2006), had a critical influence on the resulting shock-metamorphic products.

Of bearing on this question are the abundance and orientations of PDFs and the nature of other optical properties in quartz from the impact deposits. As discussed above, the quartz PDFs documented in this study and reported elsewhere from Bosumtwi impactites are more typical of those planar microstructures documented from crystalline-target impact

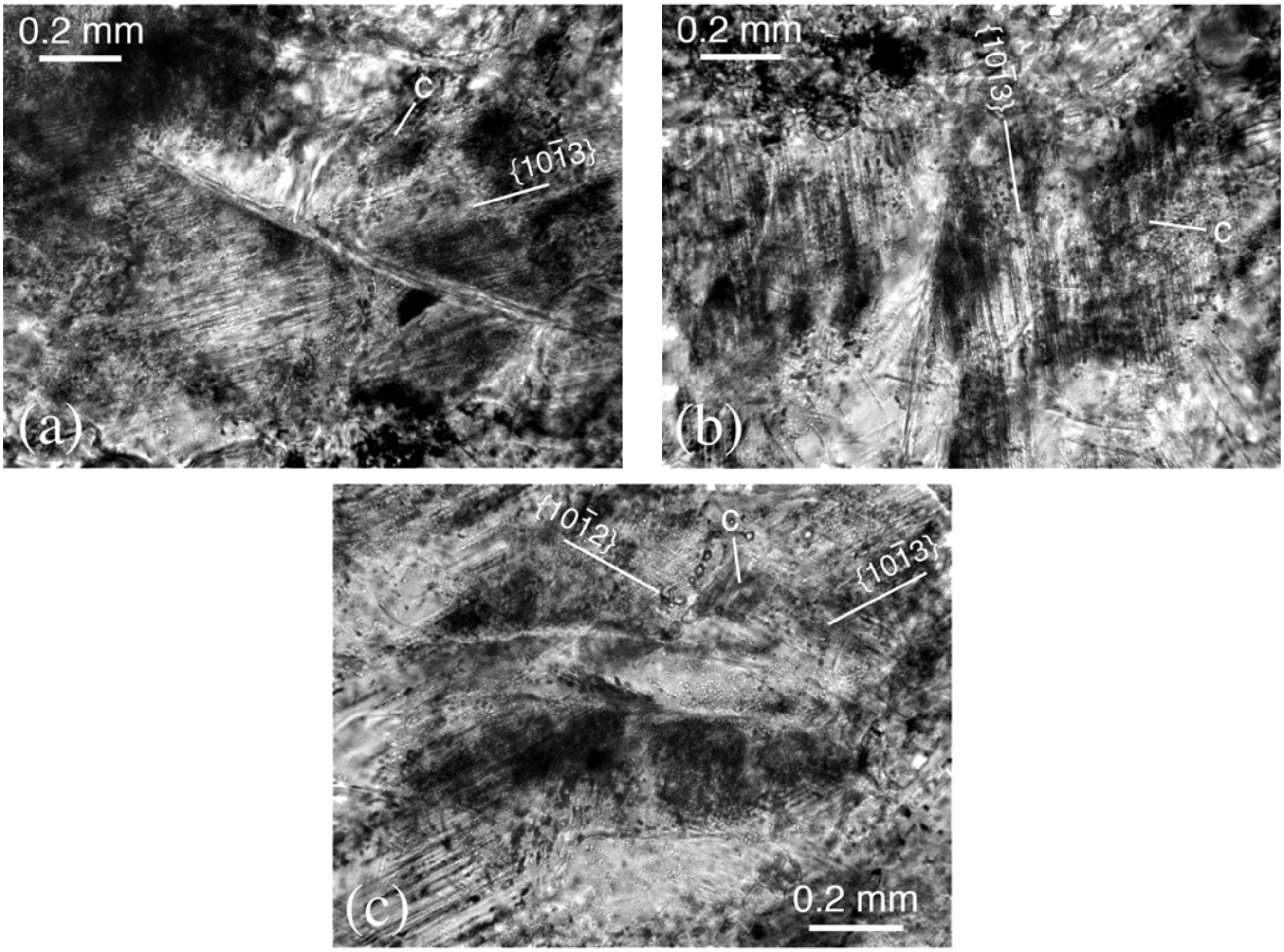

Fig. 13. Thin section photomicrographs of decorated PDFs and toasted regions in quartz, sample BOS-3, polymict lithic breccia, upper impactite unit, drill core LB-07A; plane-polarized light. a) Two areas containing a highly decorated PDF set, with $\omega\{10\bar{1}3\}$ orientation, which is developed from a prominent, subplanar fracture cross-cutting the grain interior; c-axis is indicated. Note occurrence of common toasting in association with PDFs. b) Variably decorated PDF set, orientated parallel to $\omega\{10\bar{1}3\}$, which is partly controlled by prominent subplanar fracture cutting vertically through grain; c-axis is indicated. Patchy, dark, inclusion-rich toasted regions are concentrated along PDFs. c) Highly shocked grain, with variably decorated PDFs parallel to $\omega\{1013\}$ and $\pi\{10\bar{1}2\}$ orientations; c-axis indicated. Toasted regions appear to occur preferentially within areas also containing greatest concentrations of the most highly decorated PDFs.

events. This suggests, at least from the perspective of quartz petrography, that the Tarkwaian and Birimian Supergroup metasedimentary rocks behaved more like a crystalline target than like a sedimentary one. However, the abundant inclusions, decorations, and toasting documented in the Bosumtwi shocked quartz probably attest to a water- or volatile-rich target (cf. Ferrière et al. 2007). A water-rich target environment might also speed post-impact recrystallization and annealing of glass in quartz grains, favoring the development of decorations and toasting (Whitehead et al. 2002), as well as facilitating larger scale, possible hydrothermal post-impact alteration of impact melt, finely comminuted rock particles, and unstable mineral and lithic grains into clays, which are an abundant component of the Bosumtwi impactites (cf. Boamah and Koeberl 2006; Petersen et al. 2006, 2007; Coney et al. 2007; Ferrière et al. 2007).

CONCLUSIONS

1. Standard and U-stage optical microscopic and microRaman spectroscopic analyses of quartz in polymict lithic breccia and suevite in the upper impactite interval of drill core LB-07A demonstrate pervasive but heterogeneous evidence of shock metamorphism, including phenomena related to a) deformation, such as abundant planar microstructures, grain mosaicism, and reduced birefringence, b) phase transformations, such as rare diaplectic quartz glass and very rare coesite, c) melting, such as isolated, isotropic, colorless to dark, glassy and devitrified vesicular melt grains, and d) secondary features, such as abundant, variable decoration of planar microstructures and patchy grain toasting.

2. Common to abundant PDFs in quartz, which occur in 1–4 sets per grain, are dominated by $\omega\{10\bar{1}3\}$-equivalent crystallographic orientations, although significant percentages of $\pi\{10\bar{1}2\}$ and other higher index orientations also occur; notably, *c*(0001) planes are relatively rare. In contrast to impactites deposited outside of the crater, the LB-07A upper impactite shocked quartz population contains a higher relative percentage of grains with 1 PDF set per grain, a lower relative percentage of grains with 3 PDF sets per grain, a lack of grains with 5 PDF sets per grain, a higher relative percentage of $\omega\{10\bar{1}3\}$ PDF orientations, and a lower relative percentage of $\pi\{10\bar{1}2\}$ PDF orientations.
3. The PDF orientations and abundance recorded in quartz grains within the LB-07A upper impactite sequence match most closely the PDF populations reported from other documented crystalline target-rock impact sites; this observation has implications for modeling the impact behavior of the Tarkwaian and Birimian metasedimentary rocks that comprise most of the target.
4. The high-pressure SiO_2 polymorph coesite, previously documented only in suevite outside of the crater, is now verified by microRaman spectrometry to occur within crater-filling suevite of the LB-07A upper impactite interval.
5. Distribution of melt-bearing suevite within the LB-07A upper impactite interval indicates in general that shock-metamorphic levels increase downcore. However, the occurrence of relatively common quartzite clasts and the presence of the most abundant shocked quartz near the top of the core suggest that shocked quartz-rich fallout, possibly derived from shallower target depths, could be an important component of the uppermost impactites. If this observation is valid, it may evidence two genetically distinct sequences comprising the upper-crater fill—a lower portion characterized by more locally derived lithic clasts and melt grains, transitional to monomict lithic breccia below, and a thinner upper portion containing a more significant component of ejected, ballistically transported target debris.
6. Estimation of the maximum shock pressures indicated by altered quartz, coesite, and melt in the upper impactite interval are consistent with shock barometry estimates from samples elsewhere in the LB-07A sequence and from the LB-08A drill core. A widespread maximum shock pressure of at least 20 GPa is evidenced; rarely, shock pressures exceeded 30 GPa and, more rarely, 45–50 GPa. Overall, the shock pressures recorded in the LB-07A drill core are significantly lower than those reported from suevite outside of the crater rim.
7. The abundance and orientations of PDFs in shocked quartz, the relatively high abundances of decorated planar microstructures and grain toasting in the quartz, and the nature and distribution of melt within suevite all point towards a water- or volatile-rich Bosumtwi impact target-rock sequence; furthermore, the quartz PDF orientations indicate that the target probably behaved primarily as a crystalline solid under shock-metamorphic conditions.

Acknowledgments–Drilling at Lake Bosumtwi was supported by the International Continental Scientific Drilling Program (ICDP), the U.S. NSF-Earth System History Program under grant no. ATM-0402010, the Austrian FWF (project P17194-N10), the Austrian Academy of Sciences, and the Canadian NSERC. Drilling operations were performed by DOSECC. Local help by the Geological Survey Department (Accra) and KNUST (Kumasi), Ghana, was invaluable. The University of Northern Colorado Sponsored Programs Office provided partial funding to Morrow. E. Libowitzky, Institute of Mineralogy and Crystallography, University of Vienna, is gratefully acknowledged for his assistance with the microRaman spectroscopic analyses. Appreciation is also given to C. Koeberl and W. U. Reimold for providing helpful discussions and for encouraging this contribution to the project. J. W. Horton, Jr., K. R. Evans, E. Libowitzky, and C. Koeberl are thanked for their critical and helpful reviews of the manuscript.

Editorial Handling—Dr. Christian Koeberl

REFERENCES

Alexopoulos J. S., Grieve R. A. F., and Robertson P. B. 1988. Microscopic lamellar deformation features in quartz: Discriminative characteristics of shock-generated varieties. *Geology* 16:796–799.

Artemieva N. 2007. Possible reasons of shock melt deficiency in the Bosumtwi drill cores. *Meteoritics & Planetary Science* 42. This issue.

Artemieva N., Karp T., and Milkereit B. 2004. Investigating the Lake Bosumtwi impact structure: Insight from numerical modeling. *Geochemistry Geophysics Geosystems* 5:1–20.

Barnes V. E. 1961. Tektites. *Scientific American* 205:58–65.

Boamah D. and Koeberl C. 2002. Geochemistry of soils from the Bosumtwi impact structure, Ghana, and relationship to the radiometric airborne geophysical data. In *Meteorite impacts in Precambrian shields*, edited by Plado J. and Pesonen L. J. Impact studies, vol. 2. Heidelberg-Berlin: Springer. pp. 211–255.

Boamah D. and Koeberl C. 2003. Geology and geochemistry of shallow drill cores from the Bosumtwi impact structure, Ghana. *Meteoritics & Planetary Science* 38:1137–1159.

Boamah D. and Koeberl C. 2006. Petrographic studies of "fallout" suevite from outside the Bosumtwi impact crater, Ghana. *Meteoritics & Planetary Science* 41:1761–1774.

Bohor B. F., Modreski P. J., and Foord E. E. 1987. Shocked quartz in the Cretaceous-Tertiary boundary clays: Evidence for a global distribution. *Science* 236:705–709.

Boyer H., Smith D. C., Chopin C., and Lasnier B. 1985. Raman microprobe (RMP) determinations of natural and synthetic coesite. *Physics & Chemistry of Minerals* 12:45–48.

Carter N. L. 1965. Basal quartz deformation lamellae—A criterion for recognition of impactites. *American Journal of Science* 263: 786–806.

Chao E. C. T. 1968. Pressure and temperature histories of impact metamorphosed rocks—Based on petrographic observations. In *Shock metamorphism of natural materials*, edited by French B. M. and Short N. M. Baltimore: Mono Book Corporation. pp. 135–158.

Coney L., Reimold W. U., Koeberl C., and Gibson R. L. 2006. Mineralogical and geochemical investigations of impact breccias in the ICDP borehole LB-07A, Bosumtwi impact structure, Ghana (abstract #1279). 37th Lunar and Planetary Science Conference. CD-ROM.

Coney L., Gibson R. L., Reimold W. U., and Koeberl C. 2007. Lithostratigraphic and petrographic analysis of ICDP drill core LB-07A, Bosumtwi impact structure, Ghana. *Meteoritics & Planetary Science* 42. This issue.

Dachille F., Gigl P., and Simons P. Y. 1968. Experimental and analytical studies of crystalline damage useful for the recognition of impact structures. In *Shock metamorphism of natural materials*, edited by French B. M. and Short N. M. Baltimore: Mono Book Corporation. pp. 555–583.

Dai X., Boamah D., Koeberl C., Reimold W. U., Irvine G., and McDonald I. 2005. Bosumtwi impact structure, Ghana: Geochemistry of impactites and target rocks, and search for a meteoritic component. *Meteoritics & Planetary Science* 40: 1493–1511.

Deutsch A. 2006. Lake Bosumtwi drilling project: Shock metamorphism in rocks from core BCDP-8A vs. experimental data (abstract #1327). 37th Lunar and Planetary Science Conference. CD-ROM.

Durrani S. A. and Khan H. A. 1971. Ivory Coast microtektites: Fission track age and geomagnetic reversals. *Nature* 232:320–322.

Dypvik H. and Jansa L. F. 2003. Sedimentary signatures and processes during marine bolide impacts: A review. *Sedimentary Geology* 161:309–337.

El Goresy A. 1966. Metallic spherules in Bosumtwi crater glasses. *Earth and Planetary Science Letters* 1:23–24.

El Goresy A., Fechtig H., and Ottemann T. 1968. The opaque minerals in impactite glasses. In *Shock metamorphism of natural materials*, edited by French B. M. and Short N. M. Baltimore: Mono Book Corporation. pp. 531–554.

Engelhardt W. von and Bertsch W. 1969. Shock-induced planar deformation structures in quartz from the Ries crater, Germany. *Contributions to Mineralogy and Petrology* 20:203–234.

Engelhardt W. von, Arndt J., Stöffler D., Müller W. F., Jeziorkowski H., and Gubser R. A. 1967. Diaplektische Gläser in den Breccien des Ries von Nördlingen als Anzeichen für Stosswellenmetamorphose. *Contributions to Mineralogy and Petrology* 15:93–102.

Engelhardt W. von, Hörz F., Stöffler D., and Bertsch W. 1968. Observations on quartz deformation in breccias of West Clearwater Lake, Canada, and the Ries Basin, Germany. In *Shock metamorphism of natural materials*, edited by French B. M. and Short N. M. Baltimore: Mono Book Corporation. pp. 475–482.

Ferrière L., Koeberl C., Reimold W. U., and Gibson R. L. 2006. First mineralogical observations and chemical analyses of core LB-08A from the central uplift of the Bosumtwi impact structure, Ghana: Comparison with suevite from outside the crater (abstract #1845). 37th Lunar and Planetary Science Conference. CD-ROM.

Ferrière L., Koeberl C., and Reimold W. U. 2007. Drill core LB-08A, Bosumtwi impact structure, Ghana: Petrographic and shock metamorphic studies of rocks from the central uplift. *Meteoritics & Planetary Science* 42. This issue.

Feybesse J., Billa M., Guerrot C., Duguey E., Lescuyer J., Milesi J., and Bouchot V. 2006. The Paleoproterozoic Ghanaian province: Geodynamic model and ore controls, including regional stress modeling. *Precambrian Research* 149:149–196.

French B. M. 1969. Distribution of shock-metamorphic features in the Sudbury Basin, Ontario, Canada (abstract). *Meteoritics* 4: 173–174.

French B. M. 1998. *Traces of catastrophe: A handbook of shock-metamorphic effects in terrestrial meteorite impact structures*. LPI Contribution #954. Houston, Texas: Lunar and Planetary Institute. 120 p.

French B. M. and Short N. M., editors. 1968. *Shock metamorphism of natural materials*. Baltimore: Mono Book Corporation. 644 p.

French B. M., Underwood J. R., Jr., and Fisk E. P. 1974. Shock-metamorphic features in two meteorite impact structures, southeastern Libya. *Geological Society of America Bulletin* 85: 1425–1428.

French B. M., Koeberl C., Gilmour I., Shirey S. B., Dons J. A., and Naterstad J. 1997. The Gardnos impact structure, Norway: Petrology and geochemistry of target rocks and impactites. *Geochimica et Cosmochimica Acta* 61:873–904.

French B. M., Cordua W. S., and Plescia J. B. 2004. The Rock Elm meteorite impact structure, Wisconsin: Geology and shock-metamorphic effects in quartz. *Geological Society of America Bulletin* 116:200–218.

Glass B. P. 1969. Chemical composition of Ivory Coast microtektites. *Geochimica et Cosmochimica Acta* 33:1135–1147.

Glass B. P. and Zwart P. A. 1979. The Ivory Coast microtektite strewn field: New data. *Earth and Planetary Science Letters* 43:336–342.

Grieve R. A. F. and Alexopoulos J. S. 1988. Microscopic planar features in quartz from Scollard Canyon, Alberta, and the Cretaceous-Tertiary boundary event. *Canadian Journal of Earth Sciences* 25:1530–1534.

Grieve R. A. F., Langenhorst F., and Stöffler D. 1996. Shock metamorphism in nature and experiment: II. Significance in geoscience. *Meteoritics & Planetary Science* 31:6–35.

Jones W. B. 1985a. Chemical analyses of Bosumtwi crater target rocks compared with Ivory Coast tektites. *Geochimica et Cosmochimica Acta* 49:2569–2576.

Jones W. B. 1985b. The origin of the Bosumtwi crater, Ghana—An historical review. *Proceedings of the Geological Association (London)* 96:275–284.

Jones W. B., Bacon M., and Hastings D. A. 1981. The Lake Bosumtwi impact crater, Ghana. *Geological Society of America Bulletin* 92:342–349.

Junner N. R. 1937. The geology of the Bosumtwi caldera and surrounding country. *Gold Coast Geological Survey Bulletin* 8: 1–38.

Karikari F., Ferrière L., Koeberl C., Reimold W. U., and Mader D. 2007. Petrography, geochemistry, and alteration of country rocks from the Bosumtwi impact structure, Ghana. *Meteoritics & Planetary Science* 42. This issue.

Karp T., Milkereit B., Janle J., Danuor S. K., Pohl J., Berckhemer H., and Scholz C. A. 2002. Seismic investigation of the Lake Bosumtwi impact crater: Preliminary results. *Planetary Space Science* 50:735–742.

Kieffer S. W. and Simonds C. H. 1980. The role of volatiles and lithology in the impact cratering process. *Reviews of Geophysics and Space Physics* 18:143–181.

Koeberl C. 2001. The sedimentary record of impact events. In *Accretion of extraterrestrial material throughout Earth's history*, edited by Peucker-Ehrenbrink B. and Schmitz B. New York: Kluwer Academic/Plenum Publishers. pp. 333–378.

Koeberl C. and Reimold W. U. 1995. The Newporte impact structure, North Dakota, USA. *Geochimica et Cosmochimica Acta* 59: 4747–4767.

Koeberl C. and Reimold W. U. 2005. Bosumtwi impact crater, Ghana (West Africa): An updated and revised geological map, with explanations. *Jahrbuch der Geologischen Bundesanstalt, Wien (Yearbook of the Austrian Geological Survey)* 145:31–70 (+1 map, 1:50,000).

Koeberl C., Poag C. W., Reimold W. U., and Brandt D. 1996a. Impact origin of the Chesapeake Bay structure and the source of the North American tektites. *Science* 271:1263–1266.

Koeberl C., Reimold W. U., and Brandt D. 1996b. Red Wing structure, North Dakota: Petrographical and geochemical studies, and confirmation of impact origin. *Meteoritics & Planetary Science* 31:335–342.

Koeberl C., Bottomley R. J., Glass B. P., and Storzer D. 1997. Geochemistry and age of Ivory Coast tektites and microtektites. *Geochimica et Cosmochimica Acta* 61:1745–1772.

Koeberl C., Reimold W. U., Blum J. D., and Chamberlain C. P. 1998. Petrology and geochemistry of target rocks from the Bosumtwi impact structure, Ghana, and comparison with Ivory Coast tektites. *Geochimica et Cosmochimica Acta* 62:2179–2196.

Koeberl C., Milkereit B., Overpeck J. T., Scholz C. A., Peck J., and King J. 2005. The 2004 ICDP Bosumtwi impact crater, Ghana, West Africa, drilling project: A first report (abstract #1830). 36th Lunar and Planetary Science Conference. CD-ROM.

Koeberl C., Milkereit B., Overpeck J. T., Scholz C. A., Reimold W. U., Amoako P. Y. O., Boamah D., Claeys P., Danuor S., Deutsch A., Hecky R. E., King J., Newsom H., Peck J., and Schmitt D. R. 2006a. An international and multidisciplinary drilling project into a young complex impact structure: The 2004 ICDP Bosumtwi impact crater, Ghana, drilling project—An overview (abstract #1859). 37th Lunar and Planetary Science Conference. CD-ROM.

Koeberl C., Brandstätter F., Hecht L., Reimold W. U., Peck J., and King J. 2006b. Uppermost impact fallout layer in a drillcore at the Bosumtwi impact crater (Ghana): A preliminary study (abstract #1552). 37th Lunar and Planetary Science Conference. CD-ROM.

Koeberl C., Milkereit B., Overpeck J. T., Scholz C. A., Amoako P. Y. O., Boamah D., Danuor S., Karp T., Kueck J., Hecky R. E., King J. W., and Peck J. A. 2007a. An international and multidisciplinary drilling project into a young complex impact structure: The 2004 ICDP Bosumtwi Crater Drilling Project—An overview. *Meteoritics & Planetary Science* 42. This issue.

Koeberl C., Brandstätter F., Glass B. P., Hecht L., Mader D., and Reimold W. U. 2007b. Uppermost impact fallback layer in the Bosumtwi crater (Ghana): Mineralogy, geochemistry, and comparison with Ivory Coast tektites. *Meteoritics & Planetary Science* 42. This issue.

Kolbe P., Pinson W. H., Saul J. M., and Miller E. W. 1967. Rb-Sr study on country rocks of the Bosumtwi crater, Ghana. *Geochimica et Cosmochimica Acta* 31:869–875.

Langenhorst F. 2002. Shock metamorphism of some minerals: Basic introduction and microstructural observations. *Bulletin of the Czech Geological Survey* 77:265–282.

Langenhorst F. and Deutsch A. 1998. Minerals in terrestrial impact structures and their characteristic features. In *Advanced mineralogy,* vol. 3, edited by Marfunin A. S. Berlin: Springer. pp. 95–119.

Littler J., Fahey J. J., Dietz R. S., and Chao E. C. T. 1961. Coesite from the Lake Bosumtwi crater, Ashanti, Ghana (abstract). GSA Special Paper #68. Boulder, Colorado: Geological Society of America. p. 218.

Lippolt H. J. and Wasserburg G. J. 1966. Rubidium-Strontium-Messungen an Gläsern vom Bosumtwi-Krater und an Elfenbeinküsten-Tektiten. *Zeitschrift für Naturforschung* 21A: 226–231.

Maclaren M. 1931. Lake Bosumtwi, Ashanti. *Geographical Journal* 78:270–276.

Masaitis V. L., Nazarov M. A., Badyukov D. D., and Ivanova B. A. 1991. Impact events at the Cretaceous-Tertiary boundary. *International Geology Review* 33:663–679.

McIntyre D. B. 1962. Impact metamorphism at Clearwater Lake, Quebec (abstract). *Journal of Geophysical Research* 67:1647.

Melosh H. J. 1989. *Impact cratering: A geological process*. New York: Oxford University Press. 245 p.

Milkereit B., Ugalde H., Karp T., Scholz C. A., Schmitt D., Danour S., Artemieva N., Kück J., Qian W., and L'Heureux E. 2006. Exploring the Lake Bosumtwi crater—Geophysical surveys, predictions and drilling results (abstract #1687). 37th Lunar and Planetary Science Conference. CD-ROM.

Moon P. A. and Mason D. 1967. The geology of ¼° field sheets nos. 129 and 131, Bompata S.W. and N.W. *Ghana Geological Survey Bulletin* 31:1–51.

Morrow J. R. 2006. Petrographic characteristics of quartz in suevitic impact breccia, drillcore LB-07A, Bosumtwi crater, Ghana (abstract #1258). 37th Lunar and Planetary Science Conference. CD-ROM.

Morrow J. R. and Sandberg C. A. 2001. Distribution and characteristics of multi-sourced shock-metamorphosed quartz grains, Late Devonian Alamo impact, Nevada (abstract #1233). 32nd Lunar and Planetary Science Conference. CD-ROM.

Ormö J. and Lindström M. 2000. When a cosmic impact strikes the sea bed. *Geology Magazine* 137:67–80.

Ostroumov M., Faulques E., and Lounejeva E. 2002. Raman spectroscopy of natural silica in Chicxulub impactite, Mexico. *Compte Rendus Geoscience* 334:21–26.

Pesonen L. J., Koeberl C., and Hautaniemi H. 2003. Airborne geophysical survey of the Lake Bosumtwi meteorite impact structure (southern Ghana)—Geophysical maps with descriptions. *Jahrbuch der Geologischen Bundesanstalt (Yearbook of the Austrian Geological Survey)* 143:581–604.

Petersen M. T., Newsom H. E., Moore D. M., and Nelson M. J. 2006. Preliminary X-ray diffraction evidence of hydrothermal alteration in the Bosumtwi impact crater (abstract #2099). 37th Lunar and Planetary Science Conference. CD-ROM.

Petersen M. T., Newsom H. E., Nelson M. J., and Moore D. M. 2007. Hydrothermal alteration in the Bosumtwi impact structure: Evidence from $2M_1$-muscovite, alteration veins, and fracture fillings. *Meteoritics & Planetary Science* 42. This issue.

Plado J., Pesonen L. J., Koeberl C., and Elo S. 2000. The Bosumtwi meteorite impact structure, Ghana: A magnetic model. *Meteoritics & Planetary Science* 35:723–732.

Reimold W. U., Brandt D., and Koeberl C. 1998. Detailed structural analysis of the rim of a large, complex impact crater: Bosumtwi crater, Ghana. *Geology* 26:543–546.

Reimold W. U., Koeberl C., Hough R. M., McDonald I., Bevan A., Amare K., and French B. M. 2003. Woodleigh impact structure, Australia: Shock petrography and geochemical studies. *Meteoritics & Planetary Science* 38:1109–1130.

Reimold W. U., Coney L., Koeberl C., and Gibson R. L. 2006. ICDP borehole LB-07A (Bosumtwi impact structure, Ghana): An overview and first multidisciplinary results (abstract #1350). 37th Lunar and Planetary Science Conference. CD-ROM.

Robertson P. B. and Grieve R. A. F. 1977. Shock attenuation at terrestrial impact structures. In *Impact and explosion cratering,* edited by Roddy D. J., Pepin R. O., and Merrill R. B. New York: Pergamon Press. pp. 687–702.

Robertson P. B., Dence M. R., and Vos M. A. 1968. Deformation in rock-forming minerals from Canadian craters. In *Shock metamorphism of natural materials*, edited by French B. M. and Short N. M. Baltimore: Mono Book Corporation. pp. 433–452.

Rohleder H. P. T. 1936. Lake Bosumtwi, Ashanti. *Geographical Journal* 87:51–65.

Schnetzler C. C., Pinson W. H., and Hurley P. M. 1966. Rubidium-strontium age of the Bosumtwi crater area, Ghana, compared with the age of the Ivory Coast tektites. *Science* 151:817–819.

Schnetzler C. C., Philpotts J. A., and Thomas H. H. 1967. Rare earth and barium abundances in Ivory Coast tektites and rocks from the Bosumtwi crater area, Ghana. *Geochimica et Cosmochimica Acta* 31:1987–1993.

Scholz C. A., Karp T., Brooks K. M., Milkereit B., Amoako P. Y. O., and Arko J. A. 2002. Pronounced central uplift identified in the Bosumtwi impact structure, Ghana, using multichannel seismic reflection data. *Geology* 30:939–942.

Short N. M. and Gold D. P. 1996. Petrography of shocked rocks from the central peak at the Manson impact structure. In *The Manson impact structure, Iowa: Anatomy of an impact crater*, edited by Koeberl C. and Anderson R. R. GSA Special Paper #302. Boulder, Colorado: Geological Society of America. pp. 245–265.

Stöffler D. 1971a. Coesite and stishovite in shocked crystalline rocks. *Journal of Geophysical Research* 76:5474–5488.

Stöffler D. 1971b. Progressive metamorphism and classification of shocked and brecciated crystalline rocks at impact craters. *Journal of Geophysical Research* 76:5541–5551.

Stöffler D. 1972. Deformation and transformation of rock-forming minerals by natural and experimental shock processes. I. Behavior of minerals under shock compression. *Fortschritte der Mineralogie* 49:50–113.

Stöffler D. 1984. Glasses formed by hypervelocity impact. *Journal of Non-Crystalline Solids* 67:465–502.

Stöffler D. and Langenhorst F. 1994. Shock metamorphism of quartz in nature and experiment: I. Basic observation and theory. *Meteoritics* 29:155–181.

Wagner R., Reimold W. U., and Brandt D. 2002. Bosumtwi impact crater, Ghana: A remote sensing investigation. In *Meteorite impacts in Precambrian shields*, edited by Plado J. and Pesonen L. J. Impact studies, vol. 2. Heidelberg-Berlin: Springer. pp. 189–210.

Whitehead J., Spray J. G., and Grieve R. A. F. 2002. Origin of “toasted” quartz in terrestrial impact structures. *Geology* 30:431–434.

Woodfield P. D. 1966. The geology of the ¼° field sheet 91, Fumso, N.W. Ghana. *Ghana Geological Survey Bulletin* 30:1–66.